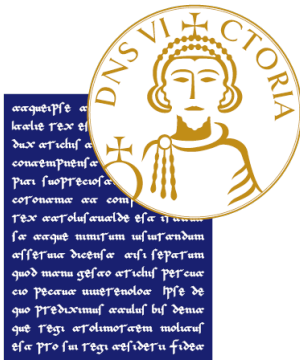


UNIVERSITY OF SANNIO

DEPARTMENT OF ENGINEERING

MASTER'S DEGREE IN

Electronics Engineering for Automation and Sensing



OPTIMAL ELECTRIC VEHICLE BATTERY MANAGEMENT FOR VEHICLE-TO-GRID: MODEL PREDICTIVE CONTROL AND REINFORCEMENT LEARNING APPROACHES

Supervisor:

Prof. Carmela Bernardo

Co-Supervisor:

Dr. Antonio Pepiciello

Candidate:

Angelo Caravella
Student ID 389000016

ACADEMIC YEAR 2024–2025

Contents

List of Acronyms	6
1 Introduction	7
1.0.1 Background and Relevance of Electric Vehicles and Vehicle-to-Grid	7
1.1 Challenges in EV Integration into the Electricity Grid and the Role of Artificial Intelligence	9
1.1.1 Objectives and Contributions of the Thesis	9
1.1.2 Research Methodology	10
1.1.3 Thesis Structure	11
2 Foundations and State of the Art in Intelligent Control for Vehicle-to-Grid Systems	13
2.1 The V2G Imperative: A Foundation of Europe's Green Transition .	13
2.2 The Optimizer's Trilemma: Navigating a Stochastic World	17
2.2.1 Sources for Energy Price Data	18
2.2.2 Buying vs. Selling: The Critical Retail-Wholesale Spread .	18
2.3 Modelling the V2G Ecosystem	19
2.3.1 The Grid-Interactive EV as a Controllable Asset	19
2.4 A New Paradigm for Control: Reinforcement Learning - Based on the work of Sutton & Barto	19
2.5 The Reinforcement Learning Problem	20
2.5.1 The Agent-Environment Interface	20
2.5.2 Goals, Rewards, and Returns	20
2.6 The Language of Learning: Markov Decision Processes	21
2.6.1 The Markov Property	22
2.6.2 Policies and Value Functions	22
2.7 The Bellman Equations	23
2.7.1 The Bellman Expectation Equation	23
2.7.2 The Bellman Optimality Equation	23
2.7.3 Generalized Policy Iteration (GPI)	23
2.8 Learning from Experience: MC and TD Methods	24
2.8.1 Monte Carlo (MC) Methods	24
2.8.2 Temporal-Difference (TD) Learning	24
2.9 Actor-Critic Architectures	25
2.10 Reward Engineering: Shaping Agent Behavior	25

2.10.1	Potential-Based Reward Shaping (PBRs)	25
2.10.2	Theoretical Foundation and Policy Invariance	26
2.10.3	Practical Implications and Design Considerations	27
2.11	Dynamic and Adaptive Rewards	27
2.11.1	Motivation and Mechanisms	28
2.12	Curriculum Learning	28
2.12.1	Specific Principles and Applications	29
2.12.2	Curriculum Learning in V2G	29
2.13	The Rise of Deep Reinforcement Learning for V2G Control	30
2.13.1	Neural Networks as Function Approximators	30
2.14	The Fundamental Role of DNNs in DRL	31
2.14.1	On-Policy Methods: Stability through Cautious Updates . .	36
2.14.2	Gradient-Free Methods: An Alternative Path	37
2.15	The Model-Based Benchmark: Model Predictive Control (MPC) .	37
2.16	MPC: Terminologies	37
2.17	Model Predictive Control Formulation	38
2.17.1	The Finite-Time Optimal Control Problem	38
2.17.2	The Receding Horizon Policy	39
2.17.3	Summary of the MPC Workflow	39
2.18	Preliminaries :General optimization problem	40
2.18.1	General optimization problem	40
2.18.2	Convex optimization problem	41
2.18.3	Convex optimization problem	42
2.18.4	Convex optimization problem: Examples	42
2.18.5	Numerical optimization	42
2.18.6	MPC: Classifications	43
2.18.7	Implicit MPC: Online Optimization	43
2.19	Improvement of the Standard Fixed-Horizon MPC Formulation .	44
2.19.1	Limitation of the Fixed-Horizon Approach	44
2.20	Improving the Formulation with Adaptive Horizon MPC (AHMPC)	45
2.20.1	The Ideal (but Impractical) AHMPC Scheme	45
2.20.2	The Practical AHMPC Algorithm	45
2.20.3	Advantages of the AHMPC Formulation	46
2.21	Further Enhancements via Learning-Based Approaches	46
2.22	Explicit MPC: Offline Pre-computation	47
2.22.1	Deep Learning for an Efficient Explicit MPC Representation	48
2.23	A Comparative Perspective on Control Methodologies	49
2.24	A Primer on Lithium-Ion Battery Chemistries and Degradation .	51
2.24.1	Fundamental Concepts and Degradation Mechanisms . . .	51
2.24.2	Key Automotive Chemistries	52
2.24.3	Voltage Profiles and the Challenge of SoC Estimation . . .	52
2.24.4	Comparative Analysis and Safety Considerations	53

3	An Enhanced V2G Simulation Framework for Robust Control	55
3.1	Core Simulator Architecture	55
3.2	A Unified Experimentation and Evaluation Workflow	57
3.2.1	Orchestration and Execution Interfaces	57
3.2.2	Scenario structure Yaml file	57
3.3	Core Simulation Parameters	58
3.4	Temporal and Contextual Settings	58
3.5	Stochastic Demand Modeling	59
3.6	Economic Framework	59
3.7	Physical Infrastructure	59
3.8	Exogenous Energy Events	60
3.9	Electric Vehicle Fleet Specification	60
3.9.1	Dual-Mode Training: Specialists and Generalists	61
3.9.2	MPC Integration and Approximation	62
3.9.3	Rigorous and Reproducible Benchmarking	62
3.9.4	Software Implementation and Project Structure	63
3.10	Core Physical Models	63
3.10.1	EV Model and Charging/Discharging Dynamics	63
3.10.2	Battery Degradation Model	64
3.10.3	Reproducible Benchmarking and Evaluation	64
3.10.4	Interactive Web-Based Dashboard	64
3.11	Evaluation Metrics	65
3.12	Simulator Implementation Details	66
3.13	Simulation Framework Components	67
3.13.1	Electric Vehicle Model (<code>ev.py</code>)	67
3.13.2	Charging Station Model (<code>ev_charger.py</code>)	69
3.13.3	Transformer Model (<code>transformer.py</code>)	70
3.13.4	Main Gym Environment (<code>ev2gym_env.py</code>)	71
3.14	Reinforcement Learning Formulation	72
3.14.1	State Space (S)	72
3.14.2	Action Space (A)	74
3.14.3	Reward Function (R)	74
3.15	Reinforcement Learning Algorithms	74
3.15.1	A History-Based Adaptive Reward for Profit Maximization .	81
3.16	Online MPC Formulation (PuLP Implementation)	85
3.16.1	Mathematical Formulation	86
3.17	Quadratic MPC Formulation (CVXPY Implementation)	87
3.18	Lyapunov-based Adaptive Horizon MPC	88

Abstract in italiano

L'adozione crescente dei **Veicoli Elettrici (EV)** in concomitanza con la sempre maggiore diffusione di **Fonti di Energia Rinnovabile (RES)** non programmabili, presenta sfide significative alla **stabilità e all'efficienza della rete elettrica**. La tecnologia **Vehicle-to-Grid (V2G)** emerge come soluzione fondamentale, trasformando gli EV da carichi passivi a **risorse energetiche flessibili** capaci di fornire vari **servizi di rete**. Questa tesi affronta il complesso **problema di ottimizzazione multi-obiettivo** della gestione intelligente di carica e scarica degli EV, che intrinsecamente implica un equilibrio tra **benefici economici, esigenze di mobilità dell'utente, preservazione della salute della batteria e stabilità della rete** in condizioni stocastiche.

Di fronte alla complessa sfida di ottimizzare la ricarica degli EV in scenari V2G, un approccio che si limita a un singolo modello di controllo, come il Deep Q-Networks (DQN), risulterebbe inadeguato. La natura del problema, caratterizzata da molteplici obiettivi contrastanti e da una profonda incertezza; richiede un'analisi comparativa e rigorosa di un'ampia gamma di strategie di controllo. Per questo motivo, la ricerca si concentra sulla valutazione di un portafoglio diversificato di algoritmi, che include numerosi modelli di Deep Reinforcement Learning (DRL), approcci euristici e il Model Predictive Control (MPC). Questo metodo consente di mappare in modo completo il panorama delle soluzioni, identificando i punti di forza e di debolezza di ciascun approccio in relazione alle diverse sfaccettature del problema V2G.

Il lavoro di tesi non si focalizza su un singolo metodo, ma adotta un approccio comparativo su larga scala perché: **non esiste una soluzione unica**: la complessità del problema V2G rende improbabile che un solo algoritmo sia ottimale in tutte le condizioni. **Si ricercano i compromessi**: l'obiettivo è comprendere i trade-off tra l'efficienza dei dati, la stabilità dell'addestramento, la robustezza all'incertezza e la complessità computazionale delle diverse famiglie di algoritmi. **La validazione è più rigorosa**: confrontare i modelli di DRL non solo tra loro ma anche con benchmark consolidati come le euristiche e l'MPC fornisce una misura molto più credibile del loro reale valore aggiunto.

Abstract

The growing adoption of **Electric Vehicles (EVs)**, combined with the increasing penetration of intermittent **Renewable Energy Sources (RESSs)**, presents significant challenges to the **stability** and **efficiency** of the power grid. The **V2G** technology emerges as a key solution, transforming EVs from passive loads into **flexible energy resources** capable of providing various **grid services**. This thesis addresses the complex **multi-objective optimization problem** of smart EV charging and discharging, which requires balancing **economic benefits**, **user mobility needs**, **battery health preservation**, and **grid stability** under stochastic conditions.

Given the complexity of optimizing EV charging in V2G scenarios, relying on a single control model is insufficient. The nature of the problem, characterized by multiple conflicting objectives (economic benefits, user needs, battery health, grid stability) and profound uncertainty, demands a rigorous comparative analysis of a wide range of control strategies.

For this reason, the research focuses on evaluating a diverse portfolio of algorithms, including numerous Deep Reinforcement Learning (DRL) models, heuristic approaches, and Model Predictive Control (MPC). This method allows for a complete mapping of the solution space, identifying the strengths and weaknesses of each approach in relation to the different facets of the V2G problem. In short, this thesis adopts a broad-spectrum comparative approach for several reasons: **No Single Solution**: the complexity of the V2G problem makes it unlikely that a single algorithm can be optimal in all conditions. **Understanding Trade-offs**: the goal is to understand the trade-offs between data efficiency, training stability, robustness to uncertainty, and the computational complexity of different algorithm families. **Rigorous Validation**: comparing DRL models not only against each other but also against established benchmarks like heuristics and MPC provides a more credible measure of their true value.

List of Acronyms

Acronym	Description
Artificial Intelligence & Control	
A2C	Advantage Actor-Critic
A3C	Asynchronous Advantage Actor-Critic
AC	Actor-Critic
AI	Artificial Intelligence
ARS	Augmented Random Search
CL	Curriculum Learning
DDPG	Deep Deterministic Policy Gradient
DQN	Deep Q-Networks
DRL	Deep Reinforcement Learning
LQR	Linear Quadratic Regulator
MILP	Mixed-Integer Linear Programming
MPC	Model Predictive Control
NN	Neural Network
PER	Prioritized Experience Replay
PPO	Proximal Policy Optimization
RL	Reinforcement Learning
SAC	Soft Actor-Critic
TD3	Twin-Delayed Deep Deterministic Policy Gradient
TQC	Truncated Quantile Critics
TRPO	Trust Region Policy Optimization
Electric Vehicles & Charging	
AFAP	As Fast As Possible (Heuristic)
ALAP	As Late As Possible (Heuristic)
CPO	Charge Point Operator
EV	Electric Vehicle
SoC	State of Charge
SoH	State of Health
V2B	Vehicle-to-Building
V2G	Vehicle-to-Grid
V2H	Vehicle-to-Home
V2V	Vehicle-to-Vehicle
VPP	Virtual Power Plant
Metrics & Technical Parameters	
AC	Alternating Current
DC	Direct Current
CC	Constant Current
CV	Constant Voltage
DoD	Depth of Discharge
MSE	Mean Square Error
RMSE	Root Mean Square Error

Chapter 1

Introduction

The global strategy for decarbonizing transport heavily relies on the shift toward electric mobility. This thesis investigates the complex challenges and opportunities arising from the large-scale integration of electric vehicles (EVs), as illustrated in Figure 1.1, into existing power grids.

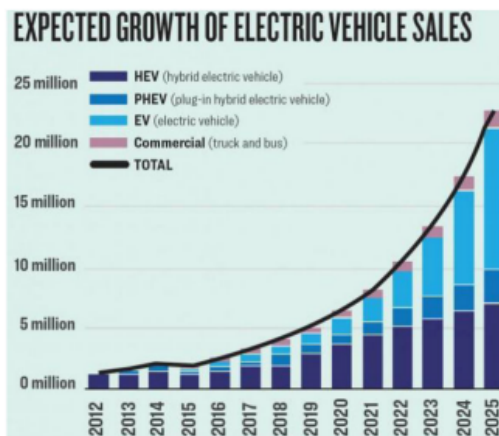


Figure 1.1: Expected growth of EV sales in the coming years (Image from: [44])

1.0.1 Background and Relevance of Electric Vehicles and Vehicle-to-Grid

The rapidly expanding Electric Vehicle market is reshaping modern mobility, offering a path to reduced carbon emissions and enhanced energy efficiency [32]. This transition is fundamental to environmental sustainability, as it lessens dependence on fossil fuels, mitigates climate change by cutting greenhouse gas emissions, and improves urban air quality. However, integrating millions of EVs into the power system is a significant challenge, threatening to intensify peak demand, strain transmission and distribution networks, and cause technical issues like voltage irregularities or line losses [32, 38].

This challenge raises a critical question: **can we transform this apparent liability into a foundational asset for grid stability?** The answer may be found in the

Vehicle-to-Grid (V2G) paradigm. V2G reimagines EVs not as passive loads, but as mobile, flexible energy assets capable of bidirectional power exchange [2]. This potential is significant, considering EVs remain parked for approximately 96% of the day, providing a vast window for grid interaction [[evertsson2024investigating](#)]. Furthermore, the rapid responsiveness of EV batteries makes them ideal for providing ancillary services like frequency regulation [2]. A growing body of research, reviewed by Qiu et al. [35] and Xie [50], suggests that intelligent, bidirectional charging can offset the negative impacts of EV integration. The central proposition of this thesis is to test this hypothesis: that through advanced control methodologies, V2G can be proven not just theoretically sound, but practically indispensable, provided its economic and grid-stabilizing benefits demonstrably outweigh costs such as battery degradation and infrastructure investment. Alongside V2G, other bidirectional power flow schemes, shown in Figure 1.2, have been proposed to enhance energy resilience:

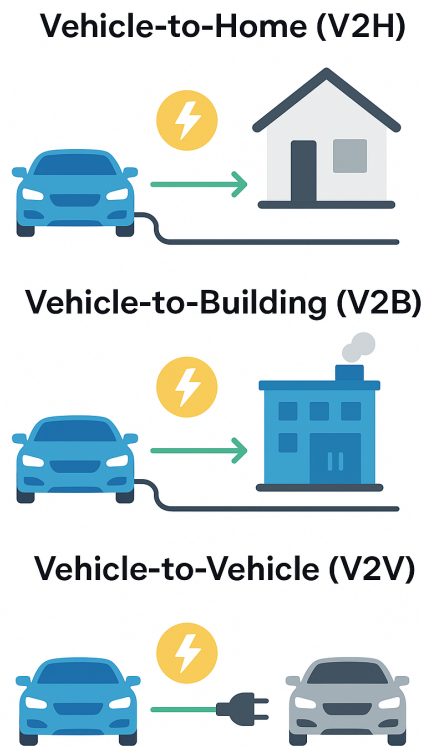


Figure 1.2: Other schemes of bidirectional power flow

1. **Vehicle-to-Home (V2H):** An EV powers a household during outages or high-cost periods, boosting domestic energy security.
2. **Vehicle-to-Building (V2B):** This concept is extended to commercial or industrial facilities, where EVs support load management and optimize energy consumption.

3. **Vehicle-to-Vehicle (V2V):** Direct power transfer between EVs provides a solution for emergency charging or resource sharing.

Collectively, these modalities underscore the versatility of EV batteries as distributed energy resources, advancing the transition to a more sustainable energy ecosystem.

1.1 Challenges in EV Integration into the Electricity Grid and the Role of Artificial Intelligence

Modern electricity systems face increasing strain from the integration of intermittent **Renewable Energy Sources (RESs)** like wind and solar. The inherent variability of RESs leads to significant power generation swings, creating supply-demand mismatches that fuel price volatility and complicate grid management. This continuous instability challenges the economic efficiency and reliability of the grid, proving difficult for conventional control frameworks to manage [32, 29]. The parallel rise of EV adoption and RES deployment has created an environment of unprecedented uncertainty and complexity. This situation makes traditional, rule-based controllers, designed for a more predictable and centralized grid, increasingly inadequate. **Is it possible, then, that a new control paradigm is needed?** The literature, as reviewed by NaXu et al. [51] and Feyijimi et al. [1], strongly suggests so, highlighting the limitations of legacy systems and framing the problem in a way that points toward data-driven methods. This shift signals a genuine paradigm change towards a *smart grid*, where adaptive, real-time, and autonomous operation is vital [51].

This has led to a surge in research focused on **Reinforcement Learning (RL)**, a paradigm that can, in theory, learn optimal control policies directly from environmental interaction without a perfect system model. While meta-heuristic algorithms have been explored, they often lack the real-time adaptability required for dynamic control [42]. The hypothesis to be tested is whether the theoretical promise of RL holds up against the engineering realities of the V2G problem. From this perspective, RL is not merely an optimization tool but an **enabling technology** for a more cognitive and robust energy infrastructure capable of navigating a decarbonized future. Within this domain, **Deep Reinforcement Learning (DRL)** has emerged as a particularly powerful approach, valued for its capacity to derive near-optimal strategies in dynamic and uncertain environments without relying on precise models or forecasts [32].

1.1.1 Objectives and Contributions of the Thesis

This thesis confronts the complex multi-objective optimization problem at the heart of Vehicle-to-Grid (V2G) systems. The overarching objective is to move beyond a purely theoretical analysis by actively developing, testing, and enhancing a high-fidelity simulation architecture. This platform serves as a digital twin to rigorously evaluate and compare advanced control strategies, balancing economic

benefits, user mobility needs, battery health, and grid stability under realistic stochastic conditions.

More than a simple review of existing literature, this work focuses on the practical implementation and validation of a V2G simulation framework in Python. This tool is leveraged to demonstrate and explore novel perspectives for training intelligent agents. The main contributions are:

- **Enhancement of a V2G Simulation Architecture:** A key contribution is the systematic testing, validation, and enhancement of the **EV2Gym** simulation framework. This work solidifies its role as a robust platform for benchmarking control algorithms and includes the development of an interactive data application using **Streamlit** for results visualization and scenario analysis.
- **Development of a Battery Degradation Calibration Algorithm:** A novel algorithm for calibrating the battery degradation model is presented. This contribution ensures that the simulation's battery health predictions are grounded in realistic parameters, increasing the fidelity of the economic and physical assessments of V2G strategies.
- **Exploration of Novel Reinforcement Learning Perspectives:** The validated simulation environment is used to investigate and implement advanced training methodologies for RL agents. A key focus is placed on techniques like **adaptive reward shaping**, where the reward function dynamically evolves during training to guide the agent towards a more holistic and robust control policy.
- **Practical Implementation and Comparison of Advanced MPC Formulations:** The thesis details the development and implementation of multiple advanced model-based controllers. This includes an **explicit MPC**, a classic **implicit MPC**, and a novel **Adaptive Horizon Model Predictive Control (AHMPC)**, all formulated in PuLP. These are benchmarked against the theoretical offline optimal controller to rigorously analyze the trade-offs inherent in real-world, online deployment with limited future information.

1.1.2 Research Methodology

The research was guided by a central question: how can the economic profit of Vehicle-to-Grid (V2G) operations be maximized without imposing undue costs in terms of battery degradation or creating instability by overloading local grid infrastructure?

The initial phase involved an extensive literature review using Google Scholar to identify state-of-the-art V2G control strategies and their inherent trade-offs. This was followed by an empirical phase centered on the simulation framework detailed in Chapter 3. The significance of results from various control agents was continuously evaluated through a multi-faceted validation process, including comparative analysis against published benchmarks, heuristic evaluation based on acquired expertise, and grounding empirical findings in the foundational

knowledge from the literature review.

To further systematize the literature review, a quantitative analysis was performed on the collected papers using a custom Python script. This analysis produced a key visualization: a weighted word cloud (Figure 1.3), was generated from titles and abstracts, with word size corresponding to its **PageRank** score within a citation graph.

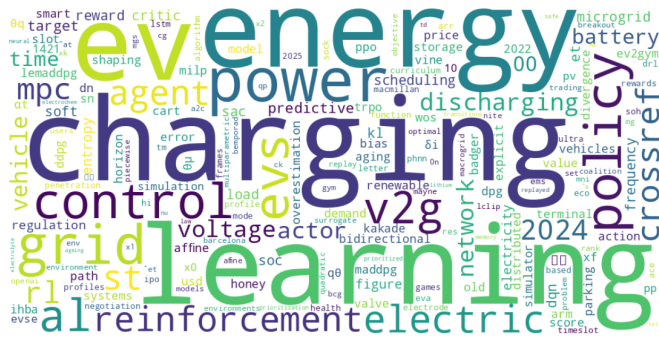


Figure 1.3: Weighted word cloud generated from the literature review, highlighting key research themes. The size of each word corresponds to its frequency and importance, derived from the PageRank analysis.

This visualization confirms the research focus, with primary terms like **Energy**, **Power**, **Grid**, and **EVs** setting the context. The equal prominence of **Learning** and **Control**, alongside strong secondary terms like **Reinforcement**, **Agent**, and **Policy**, firmly anchors the methodology in Reinforcement Learning. The inclusion of **MPC** (Model Predictive Control) highlights the central dialogue between model-free and model-based approaches explored in this thesis.

1.1.3 Thesis Structure

The remainder of this thesis is organized as follows:

- **Chapter 2: Overview of Optimal Management of EV Charging and Discharging** provides foundational knowledge on V2G technology, the complex multi-objective nature of EV charging optimization, and presents a comprehensive review of state-of-the-art research approaches.
- **Chapter 3: The V2G Simulation Framework: A Digital Twin for V2G Research** details the architecture and core models of the simulation environment. This chapter describes the enhancements made to the framework, establishing it as the central experimental platform for implementing and evaluating the control agents analyzed in this work.
- **Chapter 4: Experimental Campaign and Results Analysis** presents the main results from the comparative analysis of the different control strategies

(DRL, MPCs, heuristics). It analyzes the performance of novel training techniques, discusses the implications of the findings, and provides a detailed **sensitivity analysis** on the most critical system parameters to assess the robustness of the conclusions.

- **Bibliography** lists all cited references.

Chapter 2

Foundations and State of the Art in Intelligent Control for Vehicle-to-Grid Systems

“The green transition is the most ambitious industrial transformation ever. The region of the world that develops clean technologies first will come out on top — and I want it to be Europe.”

— URSULA VON DER LEYEN

2.1 The V2G Imperative: A Foundation of Europe’s Green Transition

Europe finds itself at the confluence of two unprecedented and deeply interlinked transformations reshaping its technological, economic, and societal landscape: the large-scale electrification of transport and a comprehensive restructuring of its energy systems. These parallel transitions involve a radical shift from internal combustion engines to battery electric vehicles and a simultaneous integration of renewable generation, grid modernization, and the deployment of advanced storage and demand-side management solutions.

These transformations are not merely aspirational targets but constitute binding legal obligations established under the **European Green Deal** and the detailed “**Fit for 55**” legislative package. These frameworks translate climate ambitions into enforceable measures aimed at reducing net greenhouse gas emissions by 55% by 2030 [12]. This policy architecture necessitates the rapid phase-out of fossil-fuelled vehicles alongside a dramatic expansion of renewable energy capacity, a goal further reinforced by the revised **Renewable Energy Directive (RED III)**, as detailed in Figure 2.1. The figure 2.1 highlights the significantly increased ambition in RED III, including a higher overall renewable energy target, a more

aggressive goal for the transport sector, and stricter requirements for traceability and legal enforceability. This escalation in policy ambition underscores the critical need for flexibility solutions like V2G to manage the grid and integrate higher shares of renewables.

	RED II (2018)	RED III (2023)
RENEWABLE ENERGY TARGET	32% by 2030	42.5% by 2030 (45% aspirational target)
TRANSPORT SECTOR TARGET	14% renewable energy	29% renewable energy, 14.5% GHG intensity reduction in transport
GHG SAVINGS THRESHOLD FOR BIOFUELS	50–65% depending on installation date	70% (existing), 80% (new installations)
MASS BALANCE TRACEABILITY	Encouraged	Mandatory
ENFORCEABILITY	Partially voluntary or indicative	Legally binding and auditable
CHAIN OF CUSTODY SYSTEMS	Not required	Required across the entire value chain
ALIGNMENT WITH OTHER EU LEGISLATION	Limited	Integrated with ETS, CBAM, and EUDR frameworks

Figure 2.1: Comparison of key targets between the Renewable Energy Directive II (RED II, 2018) and the revised RED III (2023).

Electric Vehicles (EVs) occupy a central position in this transition, simultaneously driving decarbonisation efforts while presenting complex challenges for grid stability. The initial response to mass EV adoption was characterised by concern within the power sector, viewing millions of new EVs as vast, correlated loads threatening to overwhelm distribution networks. This perspective has undergone a fundamental reassessment. EVs are now recognised not as burdens to be managed, but as essential, flexible assets for achieving Europe's energy objectives.

This conceptual shift finds its most concrete expression in **Vehicle-to-Grid (V2G)** technology, which fundamentally reimagines the role of electric vehicles within the energy system.

V2G technology transforms previously passive, unidirectional energy consumers into active, distributed, and intelligent grid resources. The underlying opportunity is substantial: private vehicles spend approximately 96% of their operational lifetime parked [14], representing an enormous, geographically distributed, and currently underutilised repository of mobile energy storage.

The transformative potential of V2G becomes apparent when individual vehicles are coordinated through centrally managed aggregation. While a single EV's contribution is modest, an orchestrated fleet can function as a unified **Virtual Power Plant (VPP)**. These software-defined power plants aggregate the collective capacity of numerous distributed energy resources, delivering grid services at scales comparable to conventional generation facilities. The rapid response characteristics of contemporary battery inverters, operating at millisecond timescales, enable these aggregated fleets to provide a comprehensive range of critical grid services. This capability is a prerequisite for maintaining stability in grids increasingly dependent on variable wind and solar generation, thereby enabling the technical and economic viability of the EU's ambitious renewable energy targets [44]. The

figure

The grid services enabled by V2G technology, many of which are illustrated in Figure ??, form the technical foundation for the smart, resilient, and decarbonised electricity system required for Europe's energy future:

Frequency Regulation: Grid stability depends on maintaining a precise equilibrium between electricity supply and demand, manifested as a stable grid frequency (50 Hz in Europe). Deviations signal imbalances that can trigger cascading failures. V2G fleets, with their rapid-response inverters, can participate in ancillary service markets like Frequency Containment Reserve (FCR) and automatic Frequency Restoration Reserve (aFRR), injecting or absorbing power within seconds to counteract deviations and prevent blackouts [2, 49].

Demand Response and Peak Shaving: By intelligently shifting charging to off-peak periods and strategically discharging during peak demand, V2G systems flatten daily load profiles. This directly mitigates the "duck curve" phenomenon (Figure 2.2) associated with high solar penetration. Such load management reduces reliance on expensive, carbon-intensive "peaker" plants and can defer or eliminate costly grid infrastructure upgrades [32, 37]. Net load is the total electricity demand minus variable renewable energy generation. The deepening "belly" of the duck during midday reflects overgeneration from solar power, while the steep "neck" in the evening represents a rapid increase in demand as solar generation fades. This steep ramp poses a significant challenge for grid operators. V2G helps mitigate this by absorbing excess energy during the day (charging) and discharging it during the evening ramp to "flatten the curve".[7]

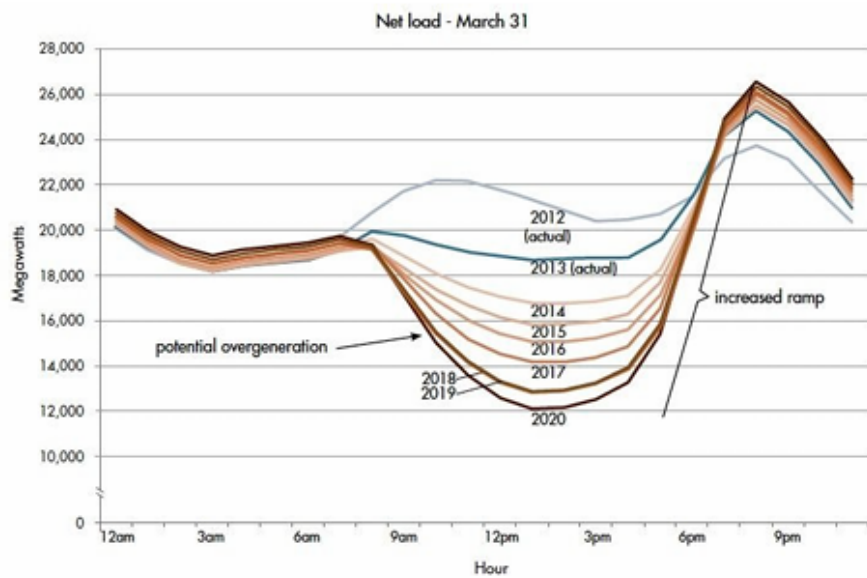


Figure 2.2: The "Duck Curve" illustrating the evolution of net load on the California grid.

Renewable Energy Integration: The most strategically significant contribution of V2G is addressing renewable energy intermittency. V2G fleets act as large-scale energy buffers, absorbing excess solar and wind generation that would otherwise

be curtailed. This stored energy is then released during periods of low generation. This mechanism directly increases the utilisation of renewable resources, supporting the integration objectives of RED III and enhancing overall system efficiency.

Economic and Market Optimization: Beyond grid stability, V2G enables sophisticated market participation. As shown in Figure ??, aggregators can deploy intelligent bidding and pricing strategies. Reinforcement learning algorithms can learn optimal policies for participating in day-ahead and intraday energy markets, maximizing revenue for both the aggregator and EV owners by capitalizing on price volatility.

User-Centric Management and Security: For V2G to succeed, it must align with user needs and address concerns. This includes optimizing charging and discharging cycles to minimize **battery degradation**, thus preserving vehicle lifespan. Furthermore, as V2G involves financial transactions and data exchange, robust **cyber security** is paramount to protect user privacy and ensure transaction security, another key domain for intelligent management systems.

This vision is being actively incorporated into European legal frameworks. The transformative **Alternative Fuels Infrastructure Regulation (AFIR, EU 2023/1804)** now mandates that new public charging infrastructure incorporate smart and bidirectional capabilities. This is supported by technical standards like **ISO 15118-20**, which specifies protocols for a "Vehicle-to-Grid Communication Interface" (V2GCI). With mandatory implementation scheduled for 2027, the necessary infrastructure is being systematically established, supported by pilot initiatives like the '**SCALE**' and '**V2G Balearic Islands**' projects.

Despite this progress, substantial obstacles to widespread V2G deployment persist:

- **Market and Economic Barriers:** A coherent, pan-European framework for compensating EV owners for grid services is still undeveloped. Accessing existing value streams is complex, and issues like the "**double taxation**" of electricity—taxing energy during both charging and discharging—create significant economic disincentives.
- **Regulatory and Grid Access Challenges:** The qualification of EV fleets as flexibility resources varies across national markets. Standardised procedures for grid interconnection, aggregator certification, and secure data exchange are needed to reduce fragmentation and simplify commercial deployment.
- **Technical and Consumer Adoption Barriers:** Consumer concerns regarding accelerated **battery degradation** and its impact on vehicle warranties are primary obstacles. Furthermore, much of the current EV and charging infrastructure lacks bidirectional capability, though this is changing with new vehicle platforms and standards.

The fundamental challenge addressed by this thesis extends beyond simply enabling V2G technology to encompass its *intelligent orchestration*. This requires

developing control strategies sophisticated enough to operate within emerging regulatory frameworks, navigate economic uncertainties, accommodate diverse user preferences, and overcome technical constraints. The objective is to unlock the substantial potential of EVs as fundamental components of Europe's energy transition while ensuring system reliability, economic viability, and user acceptance.

2.2 The Optimizer's Trilemma: Navigating a Stochastic World

While the potential of V2G technology is substantial, the management of distributed vehicular assets presents a complex control challenge. Economic viability drives aggregator decisions, yet a narrow focus on profitability alone proves insufficient for sustainable operations. Effective V2G management requires balancing three competing objectives that frequently conflict with one another. This challenge can be framed as the "V2G Optimizer's Trilemma": the concurrent pursuit of **economic profitability**, preservation of **battery longevity**, and maintenance of **user convenience**. Rather than representing a straightforward, static trade-off, this constitutes a dynamic, multi-objective optimisation challenge characterised by **stochasticity** and **uncertainty** arising from multiple, interconnected sources [47]:

Market Volatility: Wholesale electricity prices exhibit significant variability driven by unpredictable supply variations (such as sudden reductions in wind generation capacity) and demand fluctuations (including heat-driven increases in cooling demand). Effective control systems must respond to these price signals dynamically and in real-time.

Renewable Intermittency: Co-located solar and wind generation exhibit inherently variable output patterns with limited predictability. Controllers must coordinate EV fleet operations to capture available generation during surplus periods without compromising other operational objectives.

Human Behaviour: Perhaps the most challenging uncertainty source involves EV owner patterns. Arrival times, departure schedules, and required state of charge (SoC) at departure lack deterministic characteristics. Emergency departures or unexpected schedule changes represent hard, non-negotiable constraints that intelligent systems must accommodate to preserve user trust and satisfaction. This dynamic, uncertain, and multifaceted operational environment renders static, rule-based control approaches (such as "charge when price falls below threshold X, discharge when exceeding threshold Y") inadequate and brittle. More sophisticated and adaptive methodologies are required, approaches capable of learning from operational experience and making optimal decisions under conditions of significant uncertainty. Reinforcement Learning excels in precisely this domain, providing a framework for developing control policies that demonstrate robustness, adaptability, and scalability.

2.2.1 Sources for Energy Price Data

Access to reliable, real-time, and historical market data remains crucial for both control agent training in simulation environments and real-world deployment. Key public sources for European market data include:

ENTSO-E Transparency Platform: The European Network of Transmission System Operators for Electricity maintains a mandatory, open-access platform serving as a comprehensive repository of pan-European electricity market data. This includes harmonised day-ahead prices, load forecasts, and generation data, serving as the primary source for academic research through both web portal access and free RESTful API services.

National Transmission System Operators (TSOs): Many national TSOs (including Terna in Italy, National Grid in the UK, and RTE in France) publish detailed market data covering real-time frequency and imbalance prices for their respective jurisdictions.

Power Exchanges: Exchanges such as EPEX SPOT and Nord Pool constitute actual trading venues. While they represent direct price data sources, comprehensive real-time access typically requires commercial subscription services.

2.2.2 Buying vs. Selling: The Critical Retail-Wholesale Spread

A critical yet frequently overlooked aspect of V2G economics involves the distinction between EV owner charging costs and aggregator grid sales revenue.

- **Selling Price (V2G Revenue):** When EVs provide energy to the grid, revenue calculation bases on **wholesale prices** (such as day-ahead spot prices). These prices reflect pure marginal energy costs at specific times.
- **Buying Price (Charging Cost):** End consumer EV charging costs reflect **retail prices**, significantly exceeding wholesale prices due to numerous non-energy components, termed "non-commodity costs":
 - Base wholesale energy costs
 - **Grid Tariffs:** Charges for high-voltage transmission and low-voltage distribution network usage
 - **Taxes and Levies:** National or regional taxation including VAT and environmental levies applied to electricity consumption
 - **Supplier Margin:** Retail energy provider profit margins

This substantial gap between retail purchasing prices and wholesale selling prices constitutes the "retail-wholesale spread," creating the primary opportunity for profitable energy arbitrage. Successful control strategies must account for these price differentials to enable economically rational decision-making.

2.3 Modelling the V2G Ecosystem

Before examining control algorithms, establishing clear, high-fidelity models of system core components becomes essential: the electric vehicle as a controllable cyber-physical asset, and the operational environment or "scenario." The interaction between these elements defines V2G optimisation task boundaries and objectives.

2.3.1 The Grid-Interactive EV as a Controllable Asset

From a power grid perspective, electric vehicles represent sophisticated mobile energy storage devices. For V2G applications, EVs can be characterised through several key state variables and parameters:

The Battery: The core grid asset component, defined by **nominal energy capacity** (in kWh), current **State of Charge (SoC)**, and **State of Health (SoH)** representing degradation over time. Operation is constrained by **power limits** (in kW) dictating maximum charge or discharge rates, and charging/discharging **efficiencies** accounting for energy losses.

The On-Board Charger (OBC): For AC charging applications, the OBC converts grid alternating current to battery direct current. Power rating often constitutes the primary bottleneck for both charging and V2G power output.

Communication Interface: V2G participation requires vehicle-charging station (EVSE) communication capabilities. This is governed by standards including ISO 15118 and protocols such as the **Open Charge Point Protocol (OCPP)**, enabling secure information exchange required for smart and bidirectional power flow operations.

Combined with vehicle availability patterns—arrival and departure times plus user energy requirements, these characteristics transform EVs from simple loads into fully dispatchable grid resources.

2.4 A New Paradigm for Control: Reinforcement Learning - Based on the work of Sutton & Barto

"Reinforcement learning is learning what to do—how to map situations to actions—so as to maximize a numerical reward signal."

— Richard S. Sutton & Andrew G. Barto, *Reinforcement Learning: An Introduction* (2018) [43]

To address the complexities of uncertainty, multi-objective trade-offs, and dynamic systems, this work employs Reinforcement Learning (RL), a machine learning paradigm that learns optimal sequential decision-making policies through

trial-and-error interaction with an environment. Unlike traditional optimal control methods, which depend on an explicit and accurate model of the environment's dynamics, RL agents learn directly from the outcomes of their actions. This model-free approach provides significant robustness in the face of uncertainty and unmodeled dynamics.

2.5 The Reinforcement Learning Problem

The problem of reinforcement learning is formalized as the interaction between a learning **agent** and its **environment**. This interaction unfolds over a sequence of discrete time steps, $t = 0, 1, 2, \dots$.

2.5.1 The Agent-Environment Interface

At each time step t , the agent receives a representation of the environment's **state**, $S_t \in \mathcal{S}$, and on that basis selects an **action**, $A_t \in \mathcal{A}(S_t)$. One time step later, as a consequence of its action, the agent receives a numerical **reward**, $R_{t+1} \in \mathcal{R}$, and finds itself in a new state, S_{t+1} . This interaction loop forms the foundational framework of the RL problem.

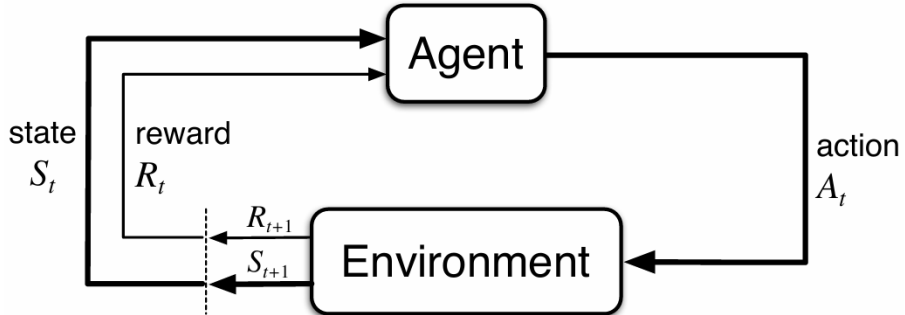


Figure 2.3: The agent-environment interaction loop in reinforcement learning [43].

2.5.2 Goals, Rewards, and Returns

The agent's objective is formalized by the **reward hypothesis**: that all goals and purposes can be framed as the maximization of the expected cumulative reward. The agent's goal is not to maximize the immediate reward, R_{t+1} , but the cumulative reward in the long run. This cumulative reward is known as the **return**, denoted G_t .

For *episodic tasks* that terminate, the return is the finite sum of future rewards. For *continuing tasks* that do not terminate, the return is defined as the discounted sum of future rewards:

$$G_t \doteq \sum_{k=0}^{\infty} \gamma^k R_{t+k+1} \quad (2.1)$$

where $\gamma \in [0, 1]$ is the **discount factor**. It determines the present value of future rewards, ensuring the infinite sum is finite and balancing immediate gratification against long-term gains. A value of $\gamma = 0$ results in a myopic agent concerned only with maximizing immediate rewards.

2.6 The Language of Learning: Markov Decision Processes

The mathematical foundation of Reinforcement Learning (RL) is the **Markov Decision Process (MDP)**. An MDP provides a formal framework for modeling decision-making in stochastic environments where outcomes are partly random and partly under the control of a decision-maker.

An MDP is formally defined as a tuple $\langle S, A, P, R \rangle$, where:

- S is a finite set of states.
- A is a finite set of actions.
- P is the state transition probability function, $P(s'|s, a)$, which represents the probability of transitioning to state s' from state s after taking action a .
- R is the reward function, $R(s, a, s')$, which is the immediate reward received after transitioning from state s to state s' as a result of action a .

A key assumption in an MDP is that the environment is fully observable, meaning the agent knows its current state with certainty. However, in many real-world scenarios, the agent may not have complete information about its state. This is where the **Partially Observable Markov Decision Process (POMDP)** comes into play.

A POMDP extends the MDP framework to situations where the agent's observations of the environment are incomplete or noisy. A POMDP is represented by a tuple $\langle S, A, P, R, \Omega, O \rangle$, which includes all the elements of an MDP plus:

- Ω is a finite set of observations the agent can receive from the environment.
- O is the observation probability function, $O(o|s', a)$, which is the probability of observing o after transitioning to state s' having taken action a .

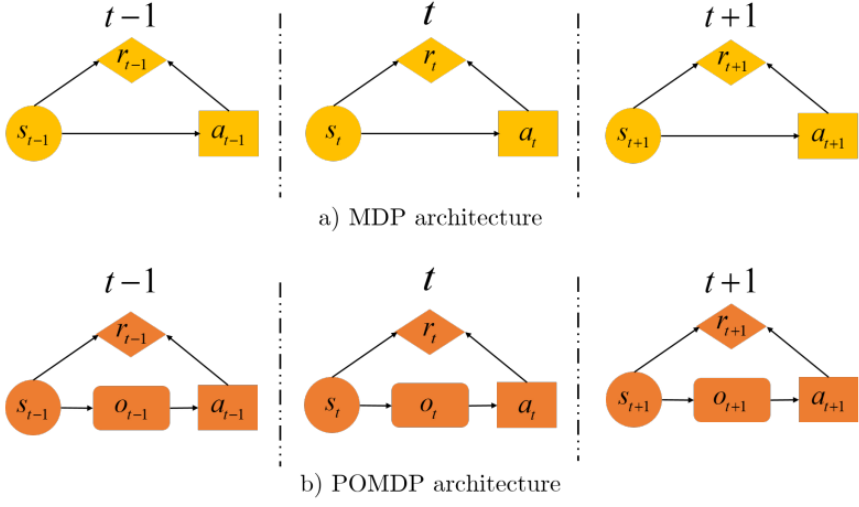


Figure 2.4: Differences between POMDP and MDP [37].

The fundamental difference between an MDP and a POMDP lies in the agent's perception of the environment's state. In an MDP, the agent directly observes the state s . In a POMDP, the agent receives an observation o and must infer a belief, which is a probability distribution over the possible states, to make a decision. As discussed in Sadeghi's work, this partial observability in POMDPs introduces a significant layer of complexity because the agent must act based on a belief state rather than a certain state.[37]

In our current discussion, we will focus on the MDP framework, assuming that the state of the environment is fully observable to the agent.

2.6.1 The Markov Property

The future is independent of the past given the present. A state signal S_t is said to have the **Markov Property** if the environment's response at time $t + 1$ depends only on the state and action at time t . The probability of transitioning to state s' and receiving reward r is independent of all previous states and actions:

$$p(s', r|s, a) \doteq \Pr\{S_{t+1} = s', R_{t+1} = r | S_t = s, A_t = a\} \quad (2.2)$$

This property is fundamental as it allows decisions to be made based solely on the current state, without needing the complete history of interaction.

2.6.2 Policies and Value Functions

The agent's learning objective is to find a good **policy**, $\pi(a|s)$, which is a mapping from states to probabilities of selecting each possible action. The goodness of a policy is assessed by its **value functions**.

- The **state-value function**, $v_\pi(s)$, is the expected return starting from state s and following policy π thereafter:

$$v_\pi(s) \doteq \mathbb{E}_\pi[G_t | S_t = s] \quad (2.3)$$

- The **action-value function**, $q_\pi(s, a)$, is the expected return starting from state s , taking action a , and thereafter following policy π :

$$q_\pi(s, a) \doteq \mathbb{E}_\pi[G_t | S_t = s, A_t = a] \quad (2.4)$$

2.7 The Bellman Equations

The Bellman equations provide a recursive decomposition that is foundational to solving MDPs. They express the value of a state in terms of the values of its successor states.

2.7.1 The Bellman Expectation Equation

For a given policy π , the state-value function must satisfy a self-consistency condition. The value of a state equals the expected immediate reward plus the discounted expected value of the next state:

$$v_\pi(s) = \sum_a \pi(a|s) \sum_{s',r} p(s', r|s, a)[r + \gamma v_\pi(s')] \quad (2.5)$$

This is the **Bellman expectation equation** for v_π . It forms the basis for policy evaluation algorithms.

2.7.2 The Bellman Optimality Equation

The ultimate goal is to find an **optimal policy**, π_* , which is a policy that achieves a higher or equal expected return than all other policies from all states. All optimal policies share the same optimal value functions, $v_*(s)$ and $q_*(s, a)$. The optimal value function for a state is the maximum expected return achievable from that state:

$$v_*(s) = \max_a \mathbb{E}[R_{t+1} + \gamma v_*(S_{t+1}) | S_t = s, A_t = a] = \max_a \sum_{s',r} p(s', r|s, a)[r + \gamma v_*(s')] \quad (2.6)$$

This is the **Bellman optimality equation**. Solving it means finding the optimal policy.

2.7.3 Generalized Policy Iteration (GPI)

Most RL algorithms can be understood within the framework of **Generalized Policy Iteration (GPI)**, as described in Chapter 4 of [43]. GPI refers to the general idea of letting two interacting processes, policy evaluation and policy improvement, work towards a common optimal solution.

- **Policy Evaluation:** Given a policy π , compute its value function v_π . This step aims to make the value function consistent with the current policy.

- **Policy Improvement:** Given a value function v , improve the policy by making it greedy with respect to v . For a given state s , the new policy will select the action a that maximizes $q_\pi(s, a)$.

These two processes compete in the short term (improving the policy makes the value function inaccurate) but cooperate in the long term to converge to the optimal policy and optimal value function. **Dynamic Programming (DP)** methods like policy iteration and value iteration are classic examples of GPI, assuming a perfect model of the environment.

2.8 Learning from Experience: MC and TD Methods

When a model of the environment is not available, we must learn from sampled experience. Chapters 5 and 6 of [43] introduce two primary model-free approaches.

2.8.1 Monte Carlo (MC) Methods

MC methods learn value functions by averaging the returns from sample episodes.

- **Principle:** An update to $V(S_t)$ is made only at the end of an episode.
- **Update Target:** The target for the update is the actual, complete return G_t .
- **Update Rule (Constant- α):** $V(S_t) \leftarrow V(S_t) + \alpha[G_t - V(S_t)]$
- **Properties:** MC methods are unbiased but can have high variance and are only applicable to episodic tasks. They do not *bootstrap*¹.

2.8.2 Temporal-Difference (TD) Learning

TD learning is a central and novel idea in RL, combining ideas from both MC and DP.

- **Principle:** TD methods update the value estimate for a state based on the observed reward and the estimated value of the successor state. They learn from incomplete episodes.
- **Update Target:** The target is an estimate of the return, called the TD Target: $R_{t+1} + \gamma V(S_{t+1})$.
- **Update Rule (TD(0)):** $V(S_t) \leftarrow V(S_t) + \alpha[R_{t+1} + \gamma V(S_{t+1}) - V(S_t)]$
- **Properties:** TD methods *bootstrap*: they update a guess from a guess. This introduces bias but often leads to lower variance and faster learning. They are naturally implemented in an online, fully incremental fashion.

¹It means that MC updates only from complete sampled returns.

2.9 Actor-Critic Architectures

The **Actor-Critic** architecture provides a powerful and widely adopted method for solving RL problems, particularly in continuous action spaces. It explicitly represents both the policy and the value function using two distinct function approximators (e.g., neural networks).

- **The Critic:** Learns a value function (e.g., $v_\pi(s)$ or $q_\pi(s, a)$). Its role is to evaluate the actor's decisions by computing the TD error:

$$\delta_t = R_{t+1} + \gamma V(S_{t+1}) - V(S_t) \quad (2.7)$$

- **The Actor:** Represents the policy, $\pi_\theta(a|s)$, parameterized by θ . It receives the current state as input and outputs an action. It uses the TD error from the critic as a learning signal to update its parameters via policy gradient methods, improving its strategy over time.

This separation of concerns allows for direct policy optimization in continuous or large action spaces while leveraging the stable learning dynamics of TD-based value estimation.

2.10 Reward Engineering: Shaping Agent Behavior

"What freedom do we have in specifying the reward function such that the optimal policy remains unchanged?"

The design of an effective reward function is arguably the most critical aspect of any Reinforcement Learning (RL) system. It serves as the primary communication channel through which designers convey desired behaviors and objectives to a learning agent. A poorly designed reward function can lead to agents learning unintended, suboptimal, or even harmful behaviors, despite successfully maximizing their assigned objective. Consequently, reward engineering has emerged as a fundamental and increasingly sophisticated discipline within modern RL, proving indispensable for the successful application of algorithms in complex, real-world scenarios [21]. The Vehicle-to-Grid (V2G) challenge, with its inherent multi-objective nature, encompassing profit maximization, assurance of user satisfaction, preservation of battery health, and maintenance of grid stability—presents particularly stringent demands on reward function design. This section investigates several advanced techniques for effectively guiding agent learning in such intricate environments.

2.10.1 Potential-Based Reward Shaping (PBRS)

Potential-Based Reward Shaping (PBRS) stands as one of the most theoretically grounded and widely adopted methods for augmenting an environment's intrinsic reward signal. The core idea behind PBRS is to supplement the original

reward, $R(s, a, s')$, received by an agent for transitioning from state s to state s' via action a , with an additional shaping term, $F(s, a, s')$. The resulting shaped reward, R' , is defined as:

$$R'(s, a, s') = R(s, a, s') + F(s, a, s') \quad (2.8)$$

The crucial characteristic of PBRS lies in the specific construction of the shaping term. To guarantee that the optimal policy remains unchanged (a property known as **policy invariance**), this shaping term must be defined as the difference in value of an arbitrary **potential function**, $\Phi : S \rightarrow \mathbb{R}$, evaluated at the successive states s and s' :

$$F(s, a, s') = \gamma\Phi(s') - \Phi(s) \quad (2.9)$$

where $\gamma \in [0, 1]$ is the discount factor of the Markov Decision Process (MDP). The potential function $\Phi(s)$ assigns a scalar value to each state, intuitively representing how "good" or "desirable" that state is. Although F is formally a function of s, a, s' , this specific potential-based form makes its value independent of the action a , which is the key insight for guaranteeing policy invariance.

2.10.2 Theoretical Foundation and Policy Invariance

The seminal work by Ng et al. [31] established the theoretical robustness of PBRS by proving a critical property: **policy invariance**.

This property guarantees that adding a potential-based shaping reward to an MDP does not alter its set of optimal policies.

In other words, **any policy that is optimal for the shaped reward function R' will also be optimal for the original reward function R , and vice versa**. This is a profound result because it ensures that while PBRS can significantly accelerate learning by providing denser and more informative feedback, it will not mislead the agent into converging on a suboptimal policy with respect to the original task. The proof of policy invariance hinges on the observation that the shaping term $F(s, s')$ can be absorbed into the value function. Specifically, if $V^*(s)$ and $Q^*(s, a)$ are the optimal value and Q-functions for the original MDP with reward R , then the optimal value and Q-functions for the shaped MDP with reward R' are given by:

$$\begin{aligned} V^{*'}(s) &= V^*(s) + \Phi(s) \\ Q^{*'}(s, a) &= Q^*(s, a) + \Phi(s) \end{aligned}$$

Since the $\Phi(s)$ term is added uniformly to all Q-values for a given state s , the action that maximizes $Q^{*'}(s, a)$ will be the same action that maximizes $Q^*(s, a)$. This preserves the optimal policy:

$$\pi^{*'}(s) = \arg \max_{a \in \mathcal{A}} Q^{*'}(s, a) = \arg \max_{a \in \mathcal{A}} (Q^*(s, a) + \Phi(s)) = \arg \max_{a \in \mathcal{A}} Q^*(s, a) = \pi^*(s)$$

This theoretical guarantee is a cornerstone of PBRS, distinguishing it from other heuristic shaping methods that might inadvertently alter the optimal policy.

2.10.3 Practical Implications and Design Considerations

The policy invariance property of PBRS offers significant practical advantages:

- **Accelerated Learning:** By providing immediate rewards for progress towards desirable states (e.g., states closer to a goal), PBRS can drastically reduce the sparsity of the reward signal, making exploration more efficient and accelerating convergence, especially in environments with delayed rewards.
- **Reduced Exploration Risk:** Agents are less likely to get stuck in local optima or exhibit undesirable behaviors during early training phases, as the shaping guides them towards more promising regions of the state space.
- **Expert Knowledge Integration:** The potential function $\Phi(s)$ can be designed using expert knowledge about the task. For instance, in a navigation task, $\Phi(s)$ could be inversely proportional to the distance to the goal, providing a positive shaping reward for moving closer to the target. In the V2G context, $\Phi(s)$ could reflect the desirability of states with high battery charge, low grid congestion, or high market prices.

Designing an effective potential function $\Phi(s)$ is key to successful PBRS. Common strategies include:

- **Distance-based Potentials:** For tasks with a clear goal, $\Phi(s)$ can be defined based on the agent's proximity to the goal state (e.g., negative Manhattan distance or Euclidean distance).
- **Subgoal-based Potentials:** In tasks requiring a sequence of steps or subgoals, $\Phi(s)$ can be constructed to provide positive potential for achieving intermediate objectives.
- **Feature-based Potentials:** For complex state spaces, $\Phi(s)$ can be a linear or non-linear function of relevant state features, allowing for more nuanced guidance.

The choice of $\Phi(s)$ should reflect the designer's intuition about what constitutes "progress" or "desirable states" without explicitly dictating the optimal actions.

2.11 Dynamic and Adaptive Rewards

In contrast to PBRS, which typically employs a static potential function throughout training, dynamic or adaptive reward functions are designed to evolve over time. This approach is particularly valuable for complex problems where the relative importance of different objectives may shift as the agent's competency develops, or as the environment itself changes.

2.11.1 Motivation and Mechanisms

Dynamic reward functions offer several advantages:

- **Addressing Evolving Objectives:** In multi-objective problems like V2G, an agent might initially struggle with basic tasks (e.g., maintaining EV charge). As it masters these, the reward function can adapt to emphasize more advanced objectives (e.g., optimizing V2G service provision while avoiding grid overloads).
- **Mitigating Conflicting Goals:** Early in training, conflicting objectives can hinder learning. Dynamic rewards can prioritize certain objectives initially, gradually introducing others as the agent becomes more capable.
- **Responding to Environmental Changes:** In non-stationary environments, an adaptive reward function can adjust its weighting of different components to reflect current conditions (e.g., higher penalty for grid overload during peak demand).

Mechanisms for implementing dynamic rewards include:

- **Time-Varying Weights:** The weights assigned to different components of a composite reward function can be adjusted based on training epochs, agent performance metrics, or predefined schedules.
- **Curiosity-Driven Rewards:** Intrinsic rewards, such as those based on novelty or prediction error, can be dynamically added or removed to encourage exploration in early stages and then faded out as the agent becomes proficient.
- **Adaptive Scaling:** Reward magnitudes can be scaled dynamically to maintain appropriate learning signals as the agent's performance improves or as the range of possible rewards changes.
- **Meta-Learning for Rewards:** More advanced techniques involve meta-learning algorithms that learn to generate or adapt reward functions based on observed agent behavior and task progress.

In the V2G context, an agent might initially receive a high reward for simply connecting to the grid and maintaining a minimum charge level. As training progresses, the reward function could dynamically incorporate larger penalties for grid instability events or higher incentives for profitable energy transactions, thereby guiding the agent towards more sophisticated and holistic V2G management strategies.

2.12 Curriculum Learning

"Can curriculum learning be considered as training the same model on different scenarios, starting with easier ones and gradually moving to more difficult ones?"

Yes, essentially, curriculum learning (CL) can be described as a strategy where the same model is trained on scenarios of increasing difficulty, starting from the easiest and progressing to the most difficult. This general idea, however, is implemented in different ways, as demonstrated by the two reference papers. The research by Pocius et al. focuses on a CL based on **task simplification**, whereas Freitag et al. propose a more specific and advanced approach based on **reward function simplification** [16, 33].

2.12.1 Specific Principles and Applications

The core principle of CL is to guide the agent's learning to prevent it from being overwhelmed by the full complexity of the final problem. The provided research offers concrete insights into how and why this approach works. **Pocius et al.** empirically compared curriculum learning, reward shaping, and visual hints in a navigation task within a Minecraft environment [33]. Their CL involved training the agent first on a simpler task (navigating a single room) before moving to a more complex one (navigating through two rooms). Their key finding was that, for their specific task, **CL** had the most significant impact on performance, surpassing the effectiveness of reward shaping. This suggests that for certain problems, structuring the learning experience through progressively harder tasks is a more powerful strategy than finely tuning the immediate reward signal [33]. On the other hand, **Freitag et al.** addressed the problem of complex reward functions with multiple and potentially conflicting terms, which often lead agents to get stuck in local optima (e.g., an agent learning to satisfy a constraint without completing the main objective) [16]. To solve this, they proposed a **two-stage reward curriculum**:

1. **Stage 1:** The agent is trained using only a subset of the reward function, termed the "base reward" (r_b), which encodes the primary task objective.
2. **Stage 2:** Once the agent has sufficiently learned the basic task, the curriculum switches to training on the full reward function, which also includes the constraint terms (r_c).

One of their key innovations is a mechanism to **automatically switch from one stage to the next** by monitoring how well the actor's policy fits the critic's Q-function. They demonstrated that this approach is particularly effective when constraints have a high weight, as it prevents the agent from being "distracted" by the constraints before understanding the main goal, leading to more stable and higher-performing final policies [16].

2.12.2 Curriculum Learning in V2G

For the V2G challenge, the two-stage reward curriculum approach proposed by Freitag et al. is particularly suitable, given the multi-objective nature of the problem. A curriculum could be structured as follows:

- 1. Stage 1: Basic Charge Management.** The agent is trained with a simplified reward function (the "base reward," r_b) that solely rewards maintaining the charge levels of electric vehicles (EVs) above a minimum threshold. All other objectives, such as grid interaction or profit, are ignored.
- 2. Stage 2: Full Optimization.** Once the agent has effectively learned to manage charging, it transitions to the full reward function. This includes the base reward plus the "constraint reward" terms (r_c), which introduce incentives for grid stability, cost minimization, and adherence to user preferences.

This structured approach, as demonstrated by Freitag et al., prevents the agent from being overwhelmed by conflicting objectives from the start, promoting the development of more robust and generalizable V2G management policies [16].

2.13 The Rise of Deep Reinforcement Learning for V2G Control

The convergence of Reinforcement Learning (RL) with the substantial representational capabilities of deep neural networks has given rise to Deep Reinforcement Learning (DRL), which currently represents the leading edge of V2G control research. The development of DRL algorithms has yielded a comprehensive toolkit, primarily divided into two main families: off-policy and on-policy methods, each exhibiting distinct operational characteristics. The following figure illustrates the evolutionary relationships between the algorithms that will be discussed, highlighting how newer ideas were built to overcome the limitations of their predecessors.

2.13.1 Neural Networks as Function Approximators

Neural networks are computational models, inspired by the interconnected structure of neurons in the human brain, designed to recognize complex patterns in data. They are comprised of layers of interconnected nodes, or *neurons*. Each neuron receives inputs, performs a weighted sum of these inputs, adds a bias, and then passes the result through a non-linear activation function to produce an output. This process can be described mathematically for a single neuron as:

$$y = f \left(\sum_{i=1}^n w_i x_i + b \right) \quad (2.10)$$

Here, y represents the neuron's output, x_i are the inputs, which are multiplied by their corresponding weights w_i . A bias, b , is added to the weighted sum. This entire result is then transformed by an activation function, f . The role of the activation function is crucial as it introduces non-linearity, enabling the network to learn and model complex, non-linear relationships in the data. Common examples of activation functions include the Sigmoid, hyperbolic tangent (tanh), and

the Rectified Linear Unit (ReLU).

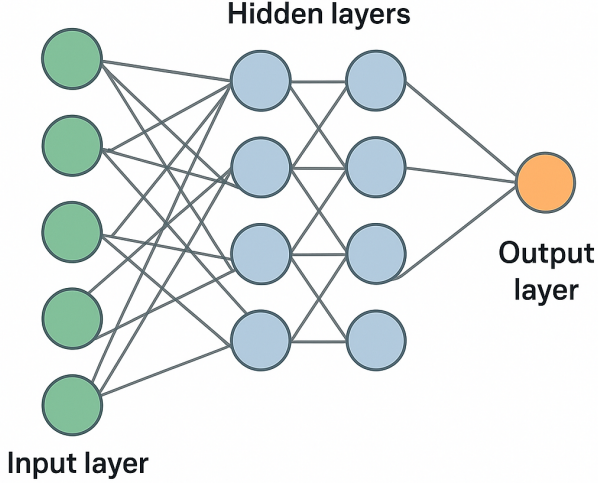


Figure 2.5: Structure of a Neural network

A neural network is constructed with an input layer 2.5, which receives the raw data, one or more *hidden layers* where the computation occurs, and an output layer that produces the final prediction or decision. **When a network contains multiple hidden layers, it is termed a *deep neural network* (DNN).** This depth allows the network to learn a hierarchical representation of features from the data, where each layer learns to identify progressively more complex patterns.

2.14 The Fundamental Role of DNNs in DRL

A prime example of this is the Deep Q-Network (DQN) algorithm, where a DNN is used to approximate the action-value function, $Q(s, a)$. The network receives the environment's state, s , as input and outputs the estimated Q-value for each possible action, a . The network is trained by minimizing a loss function, typically the mean squared error between the predicted Q-value and a target Q-value derived from the Bellman equation. The loss function is given by:

$$L(\theta) = \mathbb{E}_{(s, a, r, s') \sim D} \left[\left(r + \gamma \max_{a'} Q(s', a'; \theta^-) - Q(s, a; \theta) \right)^2 \right] \quad (2.11)$$

In this equation, θ are the weights of the neural network being trained, while θ^- are the weights of a separate, periodically updated target network used to stabilize training. The term $r + \gamma \max_{a'} Q(s', a'; \theta^-)$ is the target value, and the expectation \mathbb{E} is taken over a batch of experiences (s, a, r, s') sampled from a replay memory D . This approach enabled the agent to learn directly from high-dimensional sensory inputs, like raw pixels in Atari games, achieving human-level performance.[46]

Beyond value approximation, deep neural networks are also pivotal in policy gradient methods, where they directly parameterize the agent's policy, π . In this setup, the network, often called a *policy network*, takes a state as input and outputs a probability distribution over the possible actions. The network's weights, θ , are updated by performing gradient ascent on an objective function, $J(\theta)$, which represents the expected cumulative reward. The policy gradient theorem provides a way to update the policy parameters:

$$\nabla_{\theta} J(\theta) = \mathbb{E}_{\tau \sim \pi_{\theta}} \left[\sum_{t=0}^T \nabla_{\theta} \log \pi_{\theta}(a_t | s_t) G_t \right] \quad (2.12)$$

Here, the gradient of the objective function is calculated as the expectation of the sum of the gradients of the log probabilities of the actions taken, each weighted by the cumulative future reward, G_t . This effectively increases the probability of actions that lead to higher returns.[43]

The integration of deep neural networks has thus marked a significant leap in the quality and capability of reinforcement learning. By enabling agents to learn from high-dimensional raw data and generalize across vast state spaces, DRL has unlocked solutions to complex control problems previously considered out of reach, and it now stands as a critical tool for advancing research in V2G control systems.[34]

The convergence of RL with the substantial representational capabilities of deep neural networks has given rise to **Deep Reinforcement Learning (DRL)**, which currently represents the leading edge of V2G control research. The development of DRL algorithms has yielded a comprehensive toolkit, primarily divided into two main families: off-policy and on-policy methods, each exhibiting distinct operational characteristics. The following figure illustrates the evolutionary relationships between the algorithms that will be discussed, highlighting how newer ideas were built to overcome the limitations of their predecessors.

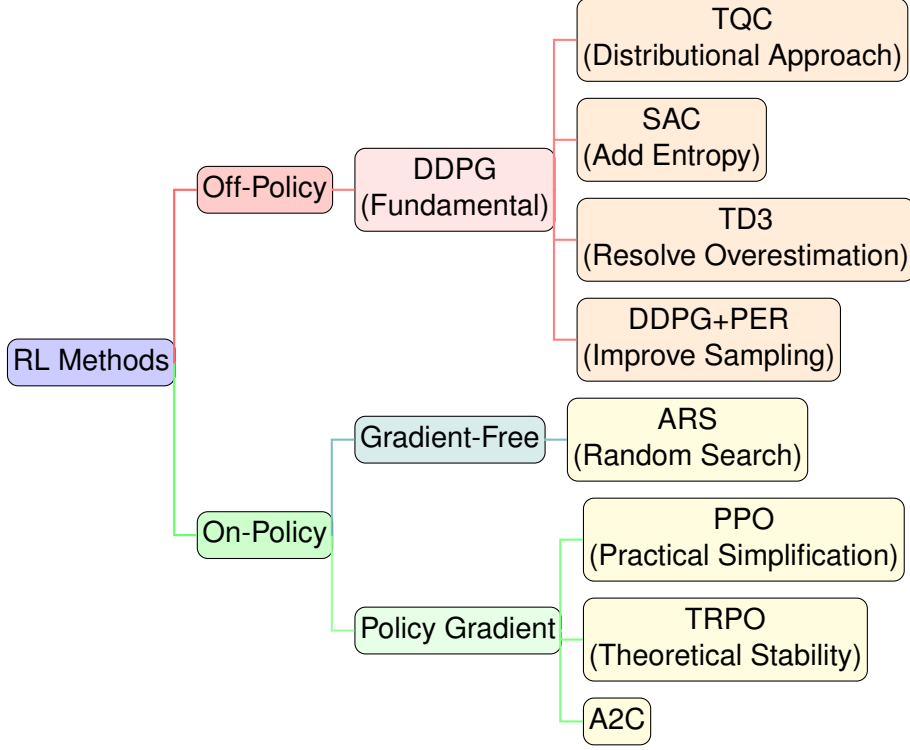


Figure 2.6: Hierarchical classification of Reinforcement Learning methods.

Off-policy algorithms distinguish themselves through their capacity to learn optimal policies from data generated by different, often more exploratory, behavioral policies. This enables them to reuse historical experiences stored in large *replay buffers*, breaking temporal correlation between experiences and achieving high sample efficiency.

A pivotal question in this domain is how to balance the exploration of new actions with the exploitation of known good actions. Off-policy methods, by their nature, are well-suited to this challenge.

Can an agent learn about the optimal way to behave while behaving
sub-optimally?

The development of algorithms like Soft Actor-Critic (SAC) [20] provides a compelling, falsifiable hypothesis: that by explicitly encouraging policy entropy, a measure of randomness, an agent can be guided to explore more broadly and avoid collapsing into a narrow, locally optimal policy. This work builds on that premise, testing whether such an approach can robustly discover profitable and stable V2G control strategies in the face of profound uncertainty.

Deep Deterministic Policy Gradient (DDPG)

A foundational algorithm that successfully extended Deep Q-Networks (DQN) to high-dimensional, continuous action spaces, DDPG represented a significant breakthrough for control problems including V2G [25]. It employs an actor-critic architecture where the actor deterministically maps states to actions. However,

practical applications often encounter substantial training instability and systematic vulnerability to **overestimation bias**, where critic networks systematically overestimate Q-values, resulting in suboptimal policy learning [32, 2].

Despite these limitations, the foundational concepts of DDPG have been successfully applied and extended in various V2G contexts. For instance, Wang et al. [48] propose a DDPG-based system for demand response management, demonstrating its potential to reduce charging costs.

But can such an approach scale to large, complex systems?

Zhang et al. [52] tackle this question by introducing a transfer learning framework built on DDPG, aiming to coordinate large-scale V2G operations with renewable energy sources. Their work puts forth a testable hypothesis: that knowledge learned in a small-scale environment can be effectively transferred to a large-scale one, thus mitigating the sample inefficiency of DRL. This thesis will implicitly test this hypothesis by evaluating the performance of DRL agents in scenarios of varying complexity.

Twin Delayed DDPG (TD3)

Developed as a direct successor to address DDPG's instabilities, TD3 introduces three key innovations that have become standard in contemporary DRL [17]. It incorporates (1) **clipped double Q-learning**, utilizing paired critic networks and selecting minimum estimates to mitigate overestimation bias; (2) **delayed policy updates**, updating actors less frequently than critics for enhanced stability; and (3) **target policy smoothing**, adding noise to target actions for learning regularization. These enhancements establish TD3 as a more robust and reliable baseline for complex V2G applications [26, 47].

The effectiveness of TD3 in V2G scheduling has been explored by multiple researchers. For example, Dou et al. [3] apply a TD3-based approach to the optimal scheduling of EV charging and discharging, demonstrating its ability to find profitable strategies. But can this profitability be achieved without negatively impacting the grid? Ding et al. [26] investigate this by using TD3 for charging scheduling while considering distribution network voltage stability. Their work provides a clear, falsifiable test of the hypothesis that a DRL agent can learn to balance its own economic incentives with the physical constraints of the power grid. This thesis builds upon this line of inquiry by incorporating explicit penalties for transformer overloads into the reward function, directly testing the agent's ability to learn this trade-off.

SAC

SAC represents a state-of-the-art off-policy algorithm for continuous control, **recognized for superior sample efficiency and stability** [19]. Its fundamental innovation involves the **maximum entropy framework**. The agent's objective is modified to maximize both expected reward and policy entropy. This entropy bonus encourages agents to act as randomly as possible while maintaining task success, promoting broader exploration, improved noise robustness, and reduced risk of poor local optima convergence.

The principle of maximum entropy, while powerful, raises a critical question:
Does encouraging random behavior compromise the safety and reliability of the system?

Gu et al. [18] directly confront this by proposing a safe reinforcement learning approach that considers battery health. Their work tests the hypothesis that one can achieve the exploration benefits of SAC while simultaneously satisfying hard constraints related to battery degradation. This is a crucial step towards making DRL a viable technology for real-world V2G deployment, and it underscores the importance of the multi-objective reward functions explored in this thesis.

Truncated Quantile Critics (TQC)

TQC addresses overestimation bias through a distributional RL approach [24]. Rather than learning single expected returns (Q-values), its critic **learns complete return probability distributions using quantile regression.**

Digression on Quantile regression:

Quantile regression is an extension of the classical linear regression model, which estimates the conditional mean of a response variable. Instead of focusing only on the mean, quantile regression estimates the conditional quantiles of the response distribution, providing a more complete statistical view. Formally, given data $\{(x_i, y_i)\}_{i=1}^n$ with predictors $x_i \in \mathbb{R}^p$ and response $y_i \in \mathbb{R}$, the τ -th conditional quantile ($0 < \tau < 1$) of Y given $X = x$ is modeled as

$$Q_Y(\tau | X = x) = x^\top \beta_\tau,$$

where β_τ are the regression coefficients associated with the quantile τ . The quantile regression estimator is obtained by solving the optimization problem:

$$\hat{\beta}_\tau = \arg \min_{\beta \in \mathbb{R}^p} \sum_{i=1}^n \rho_\tau(y_i - x_i^\top \beta),$$

where $\rho_\tau(u)$ is the so-called "check function," defined as

$$\rho_\tau(u) = u \cdot (\tau - \mathbf{1}_{\{u < 0\}}).$$

This asymmetric loss function penalizes underestimation and overestimation differently, depending on the chosen quantile τ . For example, $\tau = 0.5$ corresponds to the conditional median regression.

After learned this can be affirmed that: learning multiple return distribution quantiles and truncating the most optimistic quantile estimates before averaging, it provides a more **principled and effective method for removing primary overestimation bias sources**, frequently achieving superior performance.

Enhancement: Prioritized Experience Replay (PER)

This represents not a standalone algorithm but a crucial orthogonal modification for off-policy methods. Standard replay buffers sample past transitions uniformly. PER samples transitions based on their "importance," typically proportional to

TD error magnitude [39]. This focuses learning processes on surprising or informative experiences, significantly accelerating convergence and improving final performance.

2.14.1 On-Policy Methods: Stability through Cautious Updates

On-policy methods learn exclusively from data generated by current policies being optimized. Once data is used for updates, it is discarded. While this makes them inherently less sample-efficient than off-policy counterparts, their updates often demonstrate greater stability and reduced divergence risk.

Advantage Actor-Critic (A2C/A3C)

A2C represents a foundational synchronous, on-policy Actor-Critic algorithm. Its powerful extension, **Asynchronous Advantage Actor-Critic (A3C)**, was a landmark contribution demonstrating parallelism benefits [30]. A3C utilizes multiple parallel workers, each with individual model and environment copies. These workers interact with their environments independently, and collected gradients update a global model asynchronously. This decorrelates data streams and provides powerful stabilizing effects on learning processes.

While often considered less sample-efficient than their off-policy counterparts, on-policy methods like A2C and its variants are still actively explored in the V2G domain. For example, Chifu et al. [11] propose a Deep Q-Learning based approach for smart scheduling of EVs for demand response, which shares some of the on-policy characteristics. Their work raises the question:

Can the stability and reliability of on-policy training outweigh the sample efficiency of off-policy methods in a problem where the environment is highly stochastic? This thesis provides a direct comparison by benchmarking several state-of-the-art off-policy agents against on-policy baselines, allowing for an empirical test of this long-standing hypothesis in the DRL community.

Trust Region Policy Optimization (TRPO)

TRPO was the first algorithm to formalize policy update size constraints for guaranteed monotonic policy improvement [41]. It maximizes a "surrogate" objective function subject to policy change constraints, measured by Kullback-Leibler (KL) divergence. This creates a "trust region" within which new policies are guaranteed to improve upon previous ones, preventing catastrophic updates that can permanently derail learning. However, implementation complexity arises from second-order optimization requirements.

Proximal Policy Optimization (PPO)

PPO achieves TRPO's stability benefits and reliable performance using only first-order optimization, making it far simpler to implement and more broadly applicable [40]. It employs a novel **clipping** mechanism in its objective function to

discourage large policy updates that would move new policies too far from previous ones, effectively creating "soft" trust regions. Due to its excellent balance of performance, stability, and implementation simplicity, PPO has become a default choice for many on-policy applications.

2.14.2 Gradient-Free Methods: An Alternative Path

Augmented Random Search (ARS)

As a counterpoint to dominant gradient-based methods, ARS represents a gradient-free approach that optimizes policies directly in parameter space [27]. It operates by exploring random policy parameter perturbations and updating central policy parameter vectors based on observed performance of these perturbations. While often less sample-efficient for complex, high-dimensional problems, its extreme simplicity, scalability, and robustness to noisy rewards can make it competitive in certain domains.

2.15 The Model-Based Benchmark: Model Predictive Control (MPC)

While Deep Reinforcement Learning (DRL) offers powerful model-free approaches, model-based techniques require benchmarking against their most established and robust counterpart: **Model Predictive Control (MPC)**. MPC originated in the 1970s within the process control industry, with pioneering contributions by Richalet *et al.* [36] and Cutler and Ramaker [13]. The theoretical foundations for stability and optimality were subsequently established by Mayne and Rawlings [28]. At its core, MPC represents a proactive, forward-looking strategy that employs explicit mathematical system models to predict future evolution. At each control step, it solves a finite-horizon optimal control problem to determine the optimal control action sequence. Its primary strength, explaining widespread industrial adoption, lies in its inherent capability to handle complex system dynamics and operational constraints in a predictive manner [29].

2.16 MPC: Terminologies

Before formalizing the MPC optimization problem, it is essential to introduce the main temporal concepts that define its structure.

1. **Sampling time (T):** It is the time difference between two consecutive state measurements or control updates. It defines the discrete-time evolution of the system. In general, $T \in \mathbb{R}^+$.
2. **Time horizon (N_T):** It is the total number of time instants over which the control input is applied to the system. In general, $N_T \in \mathbb{N}$.

3. **Prediction horizon (N):** It is the number of future steps considered in the optimization process. Over this window, the system states are predicted and optimized. Typically, $N \in \mathbb{N}$ and $2 \leq N \leq N_T$.
4. **Control horizon (N_C):** It defines the number of future control moves actually optimized. Beyond this horizon, the control input is often held constant, with $N_C \leq N$.

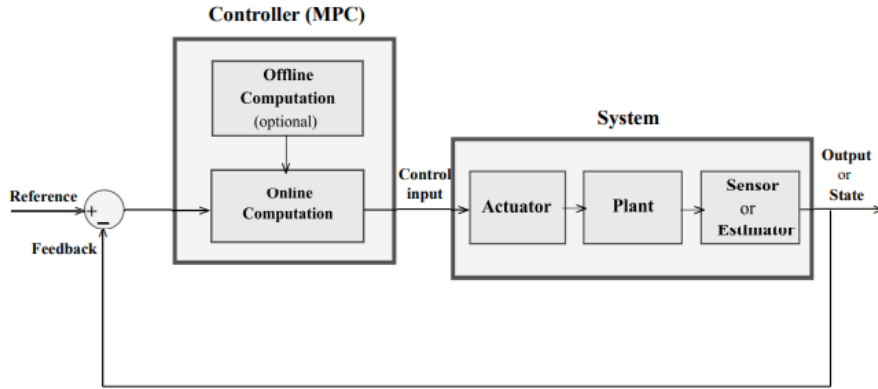


Figure 2.7: MPC: Block diagram

These concepts together define the temporal structure of MPC. At each sampling instant t , the controller predicts the system evolution over the *prediction horizon* N , optimizes a control sequence of length N_C , and applies only the first control action. The process is then repeated after T seconds, forming a closed-loop scheme known as **Receding Horizon Control (RHC)**.

2.17 Model Predictive Control Formulation

Section based on “Predictive Control for Linear and Hybrid Systems” by F. Borrelli, A. Bemporad, and M. Morari.

2.17.1 The Finite-Time Optimal Control Problem

At each time step t , given the current state measurement $x(t)$, the MPC law is defined by solving a constrained finite-time optimal control problem (FTOCP). Consider the discrete-time linear time-invariant (LTI) system:

$$x(k+1) = Ax(k) + Bu(k), \quad (2.13)$$

where $x(k) \in \mathbb{R}^n$ is the state vector and $u(k) \in \mathbb{R}^m$ is the control input.

At the current time t , using $x(t)$ as the initial state x_0 , the optimization problem is formulated as:

$$J_0^*(x(t)) = \min_{U_0} J_0(x(t), U_0) \quad (2.14)$$

subject to system and constraint dynamics, where the quadratic cost function is:

$$J_0(x(0), U_0) = x_N^\top P x_N + \sum_{k=0}^{N-1} (x_k^\top Q x_k + u_k^\top R u_k) \quad (2.15)$$

The minimization is constrained as follows for $k = 0, \dots, N - 1$:

$$x_{k+1} = Ax_k + Bu_k, \quad (2.16)$$

$$x_k \in \mathcal{X}, \quad (2.17)$$

$$u_k \in \mathcal{U}, \quad (2.18)$$

$$x_N \in \mathcal{X}_f, \quad (2.19)$$

$$x_0 = x(t). \quad (2.20)$$

Here:

- $x_k \in \mathbb{R}^n$ denotes the predicted state at step k , starting from $x_0 = x(t)$;
- $U_0 = [u_0^\top, \dots, u_{N-1}^\top]^\top \in \mathbb{R}^{mN}$ is the decision vector of future control inputs;
- $Q, P \geq 0$ are state penalty matrices, and $R > 0$ is the input penalty matrix;
- $\mathcal{X} \subseteq \mathbb{R}^n$ and $\mathcal{U} \subseteq \mathbb{R}^m$ are admissible state and input sets (often polyhedral);
- $\mathcal{X}_f \subseteq \mathbb{R}^n$ is the terminal constraint set ensuring stability.

2.17.2 The Receding Horizon Policy

The optimization yields an optimal sequence of control inputs:

$$U_0^*(x(t)) = \{u_0^*, u_1^*, \dots, u_{N-1}^*\}. \quad (2.21)$$

In the **Receding Horizon Control** (RHC) strategy, only the first control action of the optimal sequence is applied:

$$u(t) = u_0^*(x(t)). \quad (2.22)$$

At the next sampling instant $t + T$, a new measurement $x(t + T)$ is acquired, and the optimization is repeated over a shifted prediction window $[t + T, t + T + N]$. This process continues iteratively, forming a closed-loop predictive control system.

2.17.3 Summary of the MPC Workflow

1. Measure the current state $x(t)$ every sampling time T .
2. Predict system evolution over the prediction horizon N .
3. Optimize a control sequence of length N_C under system and constraint dynamics.

4. Apply the first input $u(t) = u_0^*(x(t))$.
5. Repeat at the next sampling instant.

This closed-loop iterative procedure allows MPC to handle multi-variable dynamics, input/state constraints, and future objectives within a unified optimal control framework.

2.18 Preliminaries :General optimization problem

- Optimization problem

$$\inf_{\mathbf{z}} f(\mathbf{z}) \quad \text{subject to} \quad (2.23)$$

$$\mathbf{z} \in Z \subseteq \mathbb{R}^p$$

- \mathbf{z} : Decision vector $\mathbf{z} = \begin{bmatrix} z_1 \\ z_2 \\ \vdots \\ z_p \end{bmatrix}$

- f : Cost function. Some of the basic cost functions are

1. $f(\mathbf{z}) = \mathbf{c}^T \mathbf{z}$: Linear cost function
2. $f(\mathbf{z}) = \mathbf{z}^T H \mathbf{z} + \mathbf{q}^T \mathbf{z} + r$: Quadratic cost function

- Z : Constraint set.

2.18.1 General optimization problem

- Constrained set is usually defined using linear inequalities

$$Z = \left\{ \mathbf{z} \in \mathbb{R}^2 : \begin{array}{l} z_1 \geq 0 \\ z_2 \geq 0 \\ z_1 + 2z_2 \leq 10 \\ 2z_1 + z_2 \leq 10 \end{array} \right\} \text{ which is equivalent to}$$

$$Z = \{\mathbf{z} \in \mathbb{R}^2 : F\mathbf{z} \leq \mathbf{g}\}, \quad F = \begin{bmatrix} -1 & 0 \\ 0 & -1 \\ 1 & 2 \\ 2 & 1 \end{bmatrix}, \quad \mathbf{g} = \begin{bmatrix} 0 \\ 0 \\ 10 \\ 10 \end{bmatrix}$$

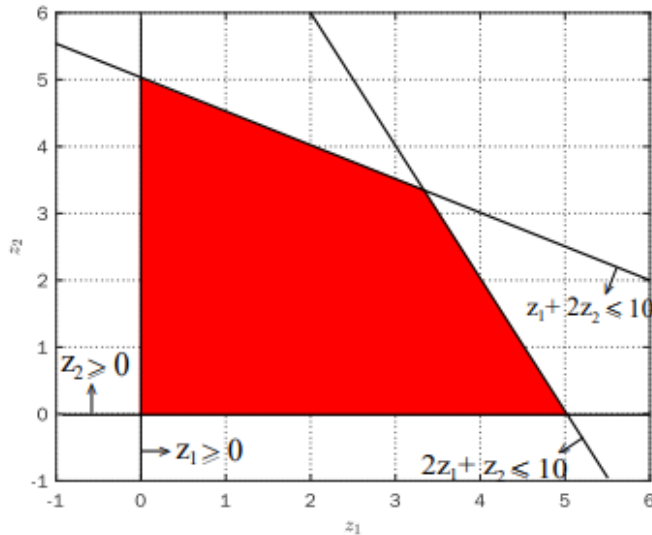


Figure 2.8: Constraint set (Polyhedron)

2.18.2 Convex optimization problem

- **Convex set:** A set $Z \in \mathbb{R}^p$ is convex if

$$\lambda \mathbf{z}_1 + (1 - \lambda) \mathbf{z}_2 \in Z \quad (2.24)$$

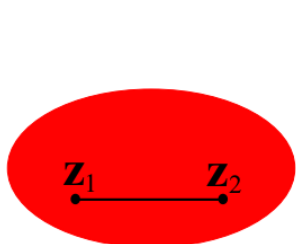
for all $\mathbf{z}_1, \mathbf{z}_2 \in Z$ and $\lambda \in [0, 1]$.

- **Convex function:** A function $f : Z \rightarrow \mathbb{R}$ is convex if Z is convex and

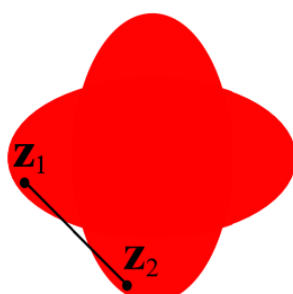
$$f(\lambda \mathbf{z}_1 + (1 - \lambda) \mathbf{z}_2) \leq \lambda f(\mathbf{z}_1) + (1 - \lambda) f(\mathbf{z}_2) \quad (2.25)$$

for all $\mathbf{z}_1, \mathbf{z}_2 \in Z$ and $\lambda \in [0, 1]$.

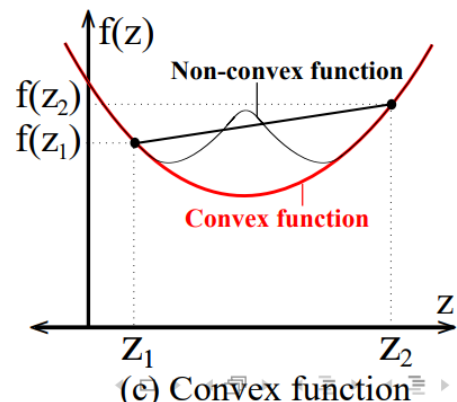
- **Convex optimization problem:** in which the cost function f is a convex function and the constraint set Z is a convex set.



(a) Convex set



(b) Non-convex set



2.18.3 Convex optimization problem

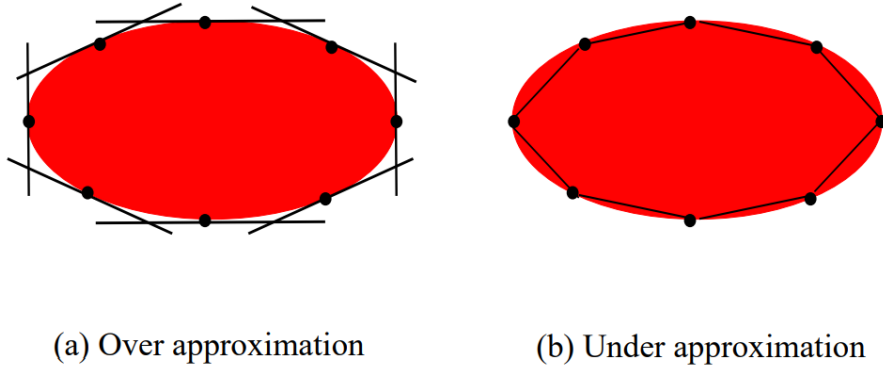


Figure 2.9: Approximating a convex set with a polytope

2.18.4 Convex optimization problem: Examples

- 1. **Linear programming problem:** is of the form

$$\begin{aligned} \inf_{\mathbf{z}} \quad & \mathbf{c}^T \mathbf{z} \quad \text{subject to} \\ & F\mathbf{z} \leq \mathbf{g} \\ & F_{eq}\mathbf{z} = \mathbf{g}_{eq} \end{aligned} \tag{2.26}$$

- 2. **Quadratic programming problem:** is of the form

$$\begin{aligned} \inf_{\mathbf{z}} \quad & \mathbf{z}^T H \mathbf{z} + \mathbf{q}^T \mathbf{z} + r \quad \text{subject to} \\ & F\mathbf{z} \leq \mathbf{g} \\ & F_{eq}\mathbf{z} = \mathbf{g}_{eq} \end{aligned} \tag{2.27}$$

2.18.5 Numerical optimization

- The two major approaches for numerical optimization
 1. **Iterative approach:** In which the elements of the decision vector are optimized together. Here the optimal decision vector is computed iteratively by starting with an initial guess which is then improved in each iterations.
 2. **Recursive approach:** In which the elements of the decision vector are optimized recursively, i.e., one at a time. The popular optimization algorithm which uses the recursive approach is the dynamic programming.

2.18.6 MPC: Classifications

- Based on the type of system model used in optimization
 1. **Linear MPC:** The system model and the constraints are linear. The cost function can be linear or quadratic which results in linear or quadratic programming problems which are convex optimization problems.
 2. **Nonlinear MPC:** The system model is nonlinear and constraints are either linear or nonlinear. The cost function is usually chosen as a linear or quadratic function which results in a nonlinear programming problem which is non-convex.
- Based on the implementation
 1. **Implicit MPC:** This also known as the traditional MPC in which the control input at each time instant is computed by solving an optimization problem online.
 2. **Explicit MPC:** In this the online computation is reduced by transferring the optimization problem offline.

2.18.7 Implicit MPC: Online Optimization

The most common formulation involves **Implicit MPC**, where constrained optimization problems are solved online at each control step. For linear systems with quadratic costs, this typically constitutes a Quadratic Program (QP). The controller's objective involves finding future control input sequences

$$U = [u_{t|t}, \dots, u_{t+N-1|t}]$$

that minimize a cost function J over a prediction horizon N . A key insight from [8] is that in this formulation, the control law is defined **implicitly** as the result of an optimization problem. There is no pre-computed algebraic function; the control action is discovered at each step through a numerical computation. This approach is powerful due to its directness but is fundamentally limited by the need to perform this computation online. The authors of [8] highlight this on page xii, stating:

“One limitation of MPC is that running the optimization algorithm on-line at each time step requires substantial time and computational resources.”

The finite-horizon optimal control problem is formulated as:

$$\min_{U_t} J(x_t, U_t) = \sum_{k=0}^{N-1} \left(x_{t+k|t}^\top \mathbf{Q} x_{t+k|t} + u_{t+k|t}^\top \mathbf{R} u_{t+k|t} \right) + x_{t+N|t}^\top \mathbf{P} x_{t+N|t} \quad (2.28)$$

where $x_{t+k|t}$ represents the predicted state at future step k based on information at time t , and \mathbf{Q} , \mathbf{R} , and \mathbf{P} are weighting matrices defining trade-offs between state

deviation and control effort. This optimization is subject to system dynamics and operational constraints:

$$x_{t+k|t} = \mathbf{A}x_{t+k|t} + \mathbf{B}u_{t+k|t} \quad (2.29)$$

$$x_{\min} \leq x_{t+k|t} \leq x_{\max} \quad (2.30)$$

$$u_{\min} \leq u_{t+k|t} \leq u_{\max} \quad (2.31)$$

At each time step t , this complete problem is solved, but only the first action of the optimal sequence, $u_{t|t}^*$, is applied to the system. The process then repeats at the next time step, $t + 1$, using new system state measurements. This feedback mechanism, known as a *receding horizon* strategy, makes MPC robust to disturbances and model mismatch [10].

2.19 Improvement of the Standard Fixed-Horizon MPC Formulation

Model Predictive Control (MPC) addresses the control of a discrete-time nonlinear system, as described in [23]:

$$x^+ = f(x, u) \quad (2.32)$$

where $x \in \mathbb{R}^n$ is the state and $u \in \mathbb{R}^m$ is the control input. The objective is to solve a finite-horizon optimal control problem at each time step. For a **fixed prediction horizon** N , the problem is formulated as finding a control sequence $u_N = (u(0), \dots, u(N-1))$ that minimizes a cost function, defined in eq. (11) of the paper as:

$$V_N(x) = \sum_{k=0}^{N-1} l(x(k), u(k)) + V_f(x(N)) \quad (2.33)$$

This minimization is subject to system dynamics, state and input constraints, and the crucial terminal constraint $x(N) \in \mathcal{X}_f$. Here, \mathcal{X}_f is a terminal set where stability is guaranteed, and $V_f(x)$ is a terminal cost that acts as a control Lyapunov function on \mathcal{X}_f [23].

2.19.1 Limitation of the Fixed-Horizon Approach

The primary drawback of this standard formulation is the static nature of the horizon N . The choice of N represents a difficult compromise. As Krener points out on page 2, "One would expect when the current state x is far from the operating point, a relatively long horizon N is needed... but as the state approaches the operating point shorter and shorter horizons can be used" [23]. A fixed horizon long enough for the worst-case scenario is computationally wasteful for the majority of the operational time, as it increases the dimensionality of the optimization problem ($m \times N$) solved online.

2.20 Improving the Formulation with Adaptive Horizon MPC (AHMPC)

The core innovation of Adaptive Horizon Model Predictive Control (AHMPC) is to make the horizon length state-dependent, adapting it online to be as short as possible while maintaining stability.

2.20.1 The Ideal (but Impractical) AHMPC Scheme

The paper first introduces an "ideal" version of AHMPC. This scheme relies on a function $N(x)$, defined as the minimum integer N for which a feasible control sequence exists that drives the state x into the terminal set \mathcal{X}_f (see Assumption 4 in [23]). The resulting optimal cost and control law are then state-dependent through this horizon:

$$V(x) = V_{N(x)}(x) \quad (2.34)$$

$$\kappa(x) = \kappa_{N(x)}(x) \quad (2.35)$$

As shown in Section II of the paper, this formulation leads to a valid Lyapunov function, confirming its stabilizing properties. However, this scheme is impractical because "in general, it is impossible to compute the function $N(x)$ " [23].

2.20.2 The Practical AHMPC Algorithm

Section III of the paper presents a practical algorithm that circumvents the need to know $N(x)$ or even the terminal set \mathcal{X}_f explicitly. The key idea is to use the terminal controller $\kappa_f(x)$ and terminal cost $V_f(x)$ to *verify online* if the chosen horizon is sufficient.

At a given state x and with a current horizon guess N , the algorithm is as follows:

- Solve and Extend:** Solve the N -horizon optimal control problem to get the trajectory $x^0(\cdot)$. Then, extend this trajectory for L additional steps using the terminal feedback law:

$$x^0(k+1) = f(x^0(k), \kappa_f(x^0(k))), \quad \text{for } k = N, \dots, N + L - 1 \quad (2.36)$$

- Verify Stability Conditions:** Check if the Lyapunov conditions, given as equations (18) and (19) in [23], hold along this extended part of the trajectory:

$$V_f(x^0(k)) \geq \alpha(|x^0(k)|) \quad (2.37)$$

$$V_f(x^0(k)) - V_f(x^0(k+1)) \geq \alpha(|x^0(k)|) \quad (2.38)$$

for $k = N, \dots, N + L - 1$. Failure to satisfy these conditions implies that the terminal state $x^0(N)$ is likely not in a region of stability.

- Adapt the Horizon:** The adaptation logic is described on page 5 of the paper:

- **If conditions hold:** The horizon N is considered sufficient. The control $u^0(0)$ is applied. At the next state x^+ , the controller attempts a shorter horizon, typically $N - 1$.
- **If conditions fail:** The horizon N is too short. The controller "increase[s] N by 1 and... solve[s] the optimal control problem over the new horizon" from the same state x [23]. This is repeated until a sufficient horizon is found.

2.20.3 Advantages of the AHMPC Formulation

This practical scheme offers significant advantages, as highlighted in the paper's conclusion:

- **Computational Efficiency:** The primary advantage is that "the AHMPC horizon length decreases as the process is stabilized thereby lessening the on-line computational burden" [23].
- **No Explicit Terminal Set:** The algorithm cleverly "proceeds without knowing the minimum horizon length function $N(x)$ and without knowing the domain of Lyapunov stability of the terminal cost $V_f(x)$ " [23]. This removes a major hurdle in traditional MPC design.

2.21 Further Enhancements via Learning-Based Approaches

While the practical AHMPC algorithm provides a significant advantage, it still relies on an iterative, trial-and-error process of increasing N when the current horizon is insufficient. This can introduce computational delays.

Modern data-driven techniques, such as Deep Reinforcement Learning (DRL), offer a path to mitigate this. DRL has proven effective for learning complex control policies for challenging problems, such as managing Electric Vehicle charging in volatile markets [32]. A hybrid approach could be envisioned where a DRL agent is trained offline to approximate the ideal horizon function $N(x)$. This learned function would provide a highly accurate initial guess for the horizon at each step, potentially eliminating the need for online iterative adjustments and combining the computational speed of a learned policy with the rigorous stability and constraint-handling framework of AHMPC.

2.22 Explicit MPC: Offline Pre-computation

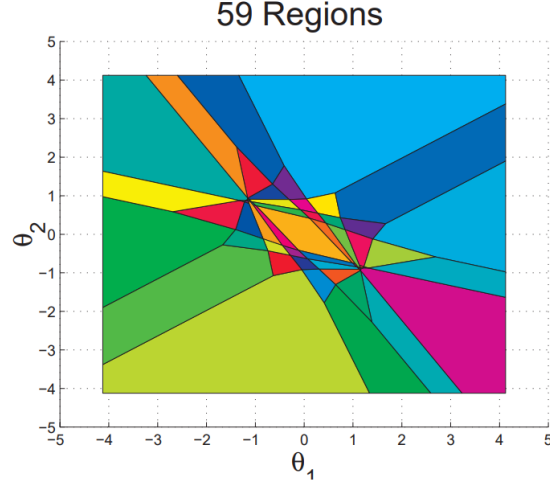


Figure 2.10: Example of a structure of a polyhedral region by Alberto Bemporad and Carlo Filippi

[5] For systems with fast dynamics or limited online computational capacity, **Explicit MPC** offers an alternative approach. The key idea is to move the computational effort entirely offline. As detailed extensively in [8], this is achieved by treating the current state x_t not as a fixed value, but as a vector of parameters. The constrained optimization problem is then solved offline for all possible initial states within a given range using **multi-parametric programming**.

The authors of [8] frame this as the main contribution of their work (Preface, page xii):

“we want to determine the [...] feedback control law $f(x)$ that generates the optimal $u_k = f(x(k))$ **explicitly** and not just **implicitly** as the result of an optimization problem.”

The result is not an online algorithm, but a pre-computed, explicit control law, $K(x_t)$, which for linear systems is a **piecewise affine (PWA) function** of the state vector x_t :

$$u^*(x_t) = \mathbf{F}_i x_t + \mathbf{g}_i \quad \text{if } x_t \in \mathcal{X}_i \quad (2.39)$$

The state space is partitioned into a set of convex polyhedral regions \mathcal{X}_i , with a unique affine control law defined for each region. Online operation is thereby reduced from solving a QP to a simple function evaluation: first, a fast lookup operation identifies which region \mathcal{X}_i the current state x_t occupies, and second, the corresponding simple affine control law is applied. This trades a very high offline computational burden and significant memory requirements for extremely fast and deterministic online execution [4, 8].

2.22.1 Deep Learning for an Efficient Explicit MPC Representation

While implicit MPC provides an optimal control action, its reliance on solving a numerical optimization problem at each sampling time makes it unsuitable for systems with fast dynamics. An alternative is Explicit MPC, where the control law—a Piecewise Affine (PWA) function of the state—is pre-computed offline. However, this approach suffers from a significant drawback: the number of polyhedral regions, and thus the memory required to store the corresponding affine laws, can grow exponentially with the prediction horizon and the number of constraints [22]. This "curse of dimensionality" severely limits its practical application, especially in memory-constrained embedded systems.

To address this challenge, the work in [22] proposes a novel approach that leverages deep learning to create a highly efficient representation of the explicit MPC law. The methodology bridges the gap between the implicit and explicit approaches by using the former to train the latter.

Training via Implicit MPC Data Generation

The core idea is to train a deep neural network to act as the explicit controller. This requires a comprehensive dataset of optimal state-action pairs, which is generated in a crucial offline phase. As detailed in [22], this is achieved by repeatedly using the **implicit MPC solver**:

1. A large number of state points ($x_{tr,i}$) are sampled from the relevant operating region of the system.
2. For each state point, the full MPC optimization problem (a Quadratic Program, or QP) is solved to find the corresponding optimal control input ($u_{tr,i}^*$). This is precisely the task an implicit MPC controller performs online.
3. The resulting pairs ($x_{tr,i}, u_{tr,i}^*$) form a large dataset that effectively maps states to their optimal control actions.

This dataset is then used to train a deep neural network via supervised learning, minimizing the error between the network's output and the optimal control actions. In essence, the computationally intensive implicit solver is used offline to "teach" a fast and compact neural network how to behave optimally.

Exact PWA Representation with Deep ReLU Networks

The power of this method stems from the theoretical insight that a deep neural network with Rectified Linear Unit (ReLU) activation functions is not merely an approximator but can, in fact, **exactly represent** the PWA function that defines the explicit MPC feedback law [22].

The foundation of this exact representation lies in two main results. First, any

scalar PWA function $K_i(x_t)$ (representing the i -th component of the control vector) can be expressed as the difference of two convex PWA functions:

$$K_i(x_t) = \gamma_i(x_t) - \eta_i(x_t) \quad (2.40)$$

Second, any convex PWA function, which can be described as the pointwise maximum of a set of affine functions, can be exactly represented by a deep ReLU network. Specifically, a convex function composed of N affine regions can be perfectly modeled by a network with width $n_x + 1$ (where n_x is the state dimension) and depth N [22]. Combining these findings, the complete multi-output MPC control law $K(x_t)$ can be exactly represented by a vector of n_u pairs of deep neural networks, where each pair models the γ_i and η_i components for a single control output:

$$K(x_t) = \begin{bmatrix} \mathcal{N}(x_t; \theta_{\gamma,1}) - \mathcal{N}(x_t; \theta_{\eta,1}) \\ \vdots \\ \mathcal{N}(x_t; \theta_{\gamma,n_u}) - \mathcal{N}(x_t; \theta_{\eta,n_u}) \end{bmatrix} \quad (2.41)$$

where \mathcal{N} denotes a deep ReLU network with its corresponding set of parameters θ . The particular advantage of using *deep* neural networks lies in their representational efficiency. While the number of parameters (and thus, the memory footprint) of a deep network grows linearly with its depth, the number of linear regions it can represent can grow exponentially [22]. This provides an inverse relationship to the problem of traditional Explicit MPC, allowing a deep network to capture an exponentially large number of control regions with only a modest, linearly growing memory cost. Consequently, this deep learning-based representation transforms the explicit MPC law into a highly compact and fast-to-evaluate form, overcoming the primary obstacle of prohibitive memory requirements and enabling the deployment of complex predictive controllers on embedded systems.

2.23 A Comparative Perspective on Control Methodologies

While DRL represents the cutting edge, contextualizing it within the broader control strategy landscape remains crucial for academic rigor. The choice between learning-based, model-free approaches and optimization-based, model-based approaches represents fundamental philosophical and practical trade-offs.

Table 2.1: Comparative Analysis: DRL vs. Model Predictive Control (MPC) for V2G

Aspect	Deep Reinforcement Learning (DRL)	Model Predictive Control (MPC)
Paradigm	Model-Free, learning-based. Learns an optimal policy (a reactive function) via trial-and-error interaction with the environment.	Model-Based, optimisation-based. Solves a constrained optimisation problem at each time step based on a system model and forecasts.
Strengths	<ul style="list-style-type: none"> Highly robust to uncertainty and unmodelled stochasticity. Does not require an explicit, accurate system model. Can learn complex, non-linear control policies. Extremely fast inference time (a single forward pass) once trained. 	<ul style="list-style-type: none"> Explicitly and rigorously handles hard constraints, providing safety guarantees. Proactive and anticipatory if forecasts are accurate. Well-established, mature, and theoretically understood.
Weaknesses	<ul style="list-style-type: none"> Can be highly sample-inefficient during the training phase. Lacks hard safety guarantees (an active and important area of research). The "black box" nature of neural network policies can make them difficult to interpret or verify. 	<ul style="list-style-type: none"> Performance is fundamentally shackled to the accuracy of the system model and external forecasts. Computationally expensive at each time step, suffering from the "curse of dimensionality" with system size. Can be brittle to unexpected forecast errors and unmodelled dynamics.
V2G Suitability	Excellent for dynamic, highly uncertain environments with complex, non-linear trade-offs and a large number of assets.	Good for problems with simple, well-defined dynamics and reliable forecasts, but struggles with the real-world stochasticity and scale of V2G.

Model Predictive Control (MPC) stands as the most powerful model-based alternative. Its primary and most compelling strength lies in its native ability to handle hard constraints, which is critical for ensuring safe operation (such as never violating transformer limits or user energy requirements). However, its performance remains fundamentally constrained by the accuracy of its internal model and forecasts of future disturbances (prices, user behavior) [15]. In practice, creating accurate, tractable models for the entire V2G domain proves nearly impossible due to non-linear battery dynamics, extreme market volatility, and the profound unpredictability of human behavior. Furthermore, as EV fleet sizes grow, optimization problem dimensionality explodes, making online computation required at each time step intractable for large fleets.

Other methods, such as **meta-heuristic algorithms** (including genetic algorithms and particle swarm optimization), are sometimes proposed. However, these are typically employed for offline scheduling and lack the real-time, reactive responsiveness required for dynamic V2G control in rapidly changing environments.

Ultimately, DRL's singular advantage lies in its ability to learn and internalize the complex, non-linear trade-offs of multi-objective V2G problems directly from data, without requiring explicit models. This makes it uniquely suited to navigating the profound uncertainties of real-world operations. While other methods

have their applications, DRL stands out as the most promising technology for deploying truly intelligent, autonomous, and scalable V2G management systems required to achieve the ambitious energy and climate objectives of the European Union.

2.24 A Primer on Lithium-Ion Battery Chemistries and Degradation

The effectiveness, safety, and economic viability of any V2G strategy remain fundamentally constrained by the physical and chemical characteristics of vehicle batteries. Battery chemistry selection dictates EV operational envelopes, influencing energy density, power capabilities, lifespan, and safety profiles. Clear understanding of these trade-offs proves essential for developing robust, realistic, and responsible control algorithms.

2.24.1 Fundamental Concepts and Degradation Mechanisms

Battery degradation is a complex and irreversible process that gradually reduces a cell's ability to store and deliver energy. It manifests primarily as capacity loss (energy fade) and as an increase in internal resistance (power fade). These phenomena are usually attributed to two categories of mechanisms: *calendar aging* and *cyclic aging* [6].

Calendar aging occurs while the battery is at rest, regardless of whether it is fully charged or nearly empty. The main mechanism behind this process is the slow growth of the **Solid Electrolyte Interphase (SEI)** layer on the graphite anode. While a thin and stable SEI layer is necessary for battery operation, its continuous thickening consumes both active lithium and electrolyte, resulting in irreversible capacity loss. The rate of SEI growth is particularly sensitive to operating conditions. High temperatures accelerate chemical reaction rates, including parasitic ones, making storage in hot environments detrimental. Similarly, high states of charge (SoC) correspond to low anode potentials, which increase the reactivity of graphite with the electrolyte and foster faster SEI growth [45]. For this reason, leaving electric vehicles stored for long periods at 100% SoC is generally discouraged.

Cyclic aging, in contrast, results from the processes that take place during charging and discharging. This form of degradation is of particular importance for V2G applications, which inherently involve frequent cycling. Several mechanisms contribute to cyclic aging. The repeated intercalation and de-intercalation of lithium ions induce mechanical stress due to the expansion and contraction of electrode materials. Over time, this stress may generate micro-cracks in electrode particles, leading to a loss of electrical contact and a reduction of active material, effects that become more severe with larger **Depths of Discharge (DoD)**. Mechanical volume changes can also compromise the integrity of the SEI layer, causing cracks that expose fresh anode surface to the electrolyte and trigger renewed SEI growth. In addition, under demanding conditions, such as very high charging rates (high

C-rates) or low temperatures, lithium ions may deposit as metallic lithium on the anode surface rather than intercalating properly. This phenomenon, known as lithium plating, is particularly harmful: it leads to rapid capacity loss and may produce dendritic structures capable of piercing the separator, thereby creating internal short circuits and serious safety hazards [6].

Both calendar and cyclic aging are unavoidable, the latter is especially critical for V2G systems. Since these applications require frequent and sometimes deep cycling, understanding and mitigating cyclic degradation is paramount to guarantee long-term system viability.

2.24.2 Key Automotive Chemistries

The EV market is dominated by several key lithium-ion battery families, primarily distinguished by cathode materials. Each chemistry presents different balances of performance characteristics.

- **Lithium Nickel Manganese Cobalt Oxide (NMC):** For years, this has been the most popular choice due to its excellent balance of energy density, power, and cycle life. The ratio of Nickel, Manganese, and Cobalt can be adjusted (such as NMC111, NMC532, NMC811) to prioritize either energy density (high Nickel) or safety and longevity (lower Nickel).
- **Lithium Nickel Cobalt Aluminum Oxide (NCA):** Offers very high specific energy (energy density by weight), enabling longer vehicle range. However, it typically comes at the cost of slightly lower cycle life and narrower safety margins compared to NMC, requiring more sophisticated thermal management.
- **Lithium Iron Phosphate (LFP):** Is rapidly gaining market share, particularly in standard-range vehicles, due to lower cost (no cobalt, an expensive and ethically contentious material) and superior safety. LFP batteries offer exceptional cycle life (often 3-4 times that of NMC/NCA) and are considered the safest common Li-ion chemistry due to high thermal stability. Their main drawback involves lower energy density.
- **Lithium Titanate Oxide (LTO):** This represents a more niche chemistry using titanate-based anodes instead of graphite. This provides exceptional safety (virtually no thermal runaway risk), extremely long cycle life (>10,000 cycles), and excellent low-temperature performance. However, very low energy density and high cost currently limit its use to specialized applications.

2.24.3 Voltage Profiles and the Challenge of SoC Estimation

The relationship between battery open-circuit voltage and SoC represents a critical, non-linear function unique to each chemistry. The derivative of cell voltage with respect to DoD, $\frac{dV_{cell}}{d(DoD)}$, constitutes a key parameter for Battery Management Systems (BMS). Steep, monotonic slopes allow BMS to accurately infer SoC

from simple voltage measurements. Conversely, flat slopes make this estimation extremely difficult.

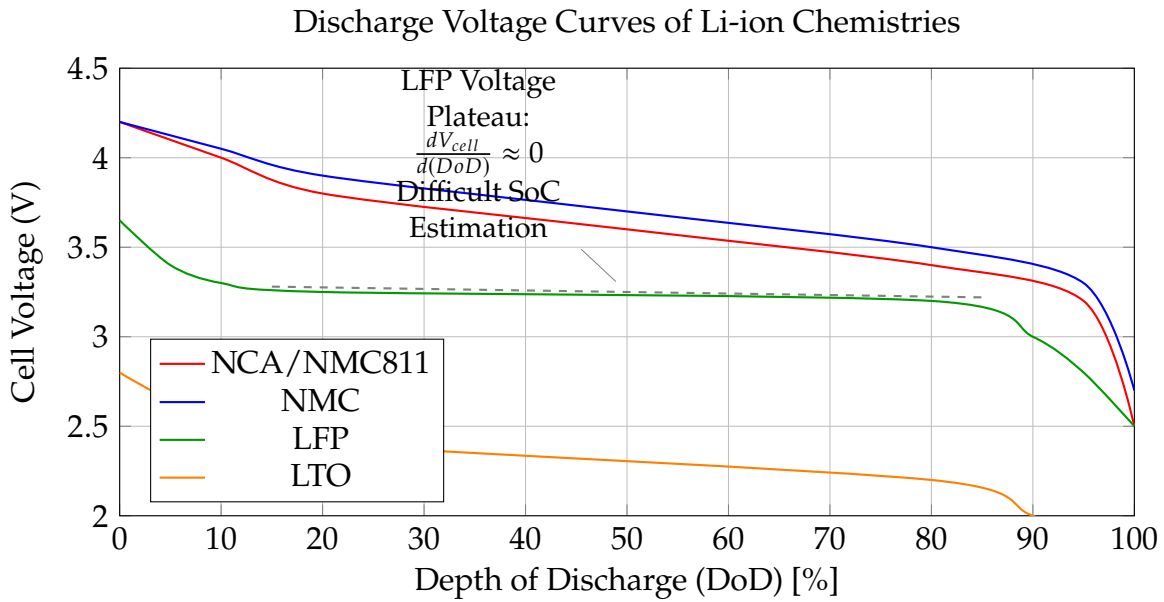


Figure 2.11: Typical discharge voltage curves for various lithium-ion chemistries. The extremely flat profile of LFP makes accurate SoC estimation challenging based on voltage alone, necessitating more complex estimation techniques like Coulomb counting and periodic recalibration.

As shown in Figure 2.11, LFP's remarkably flat voltage plateau makes it nearly impossible for BMS to determine precise SoC in the central operating range (from approximately 20% to 80%) using voltage alone. This necessitates more complex estimation techniques, such as Coulomb counting (integrating current over time), which can suffer from drift. To correct this drift, LFP-equipped vehicles require periodic full charges to 100% for BMS recalibration. This represents an important operational constraint that V2G control strategies must consider.

2.24.4 Comparative Analysis and Safety Considerations

The trade-offs between chemistries are summarized in Table 2.2. Safety remains paramount, with the primary risk being thermal runaway, a dangerous, self-sustaining exothermic reaction. This risk relates directly to cathode material chemical and thermal stability. Higher energy density generally means more energy packed into smaller mass, which can be released violently if cells are compromised. Consequently, critical temperatures for initiating thermal runaway are generally lower for higher energy density chemistries. LFP's stable phosphate-based structure makes it far more resistant to thermal runaway than nickel-based counterparts, a key reason for its growing popularity.

Table 2.2: Comparative analysis of key automotive battery chemistries, highlighting the trade-offs between performance and safety.

Metric	NCA	NMC	LFP	LTO	LCO
Energy Density (Wh/kg)	200 - 260 (Highest)	150 - 220 (High)	90 - 160 (Moderate)	60 - 110 (Low)	150-200 (High)
Cycle Life	1000 - 2000	1000 - 2500	2000 - 5000+	>10,000	500 - 1000
Safety	Good	Very Good	Excellent	Excellent	Poor
Thermal Runaway Temp (°C)	~150 - 180	~180 - 210	~220 - 270	> 250	~150

Chapter 3

An Enhanced V2G Simulation Framework for Robust Control

Developing, validating, and benchmarking advanced control algorithms for Vehicle-to-Grid (V2G) systems presents significant challenges. Real-world experimentation is often impractical due to high costs, logistical constraints, and potential risks to grid stability and vehicle hardware. A realistic, flexible, and standardized simulation environment is therefore essential. This thesis builds upon **EV2Gym**, an open-source simulator designed for V2G smart charging research [32]. The work presented here extends the original framework substantially, transforming it into a high-fidelity **digital twin** suitable not only for single-scenario optimization, but also for developing and rigorously evaluating **robust, generalist control agents**. The enhanced framework supports two complementary modes of experimentation: detailed analysis of agents specialized for a single environment, and a novel methodology for training and testing agents capable of generalizing across multiple diverse and unpredictable scenarios. This chapter presents the extended architecture, its data-driven models, and its evaluation capabilities, establishing the methodological foundation for subsequent chapters.

3.1 Core Simulator Architecture

The framework maintains the modular architecture of EV2Gym, which mirrors the key entities of a real-world V2G system. It is built on the OpenAI Gym (now Gymnasium) API, which provides a standardized agent-environment interface based on states, actions, and rewards [9].

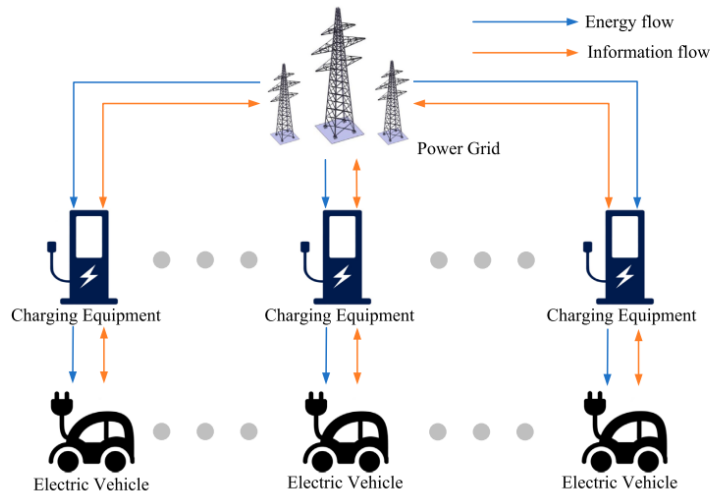


Figure 3.1: Diagram of charging and discharging scheduling for EVs. [3].

The architecture consists of several interacting components:

- **Charge Point Operator (CPO):** The central management component of the simulation, responsible for controlling the charging infrastructure and serving as the primary interface for the control algorithm (the DRL agent). The CPO aggregates system state information and dispatches control actions to individual chargers.
- **Chargers:** Digital representations of physical charging stations, configurable by type (AC/DC), maximum power, and efficiency. This enables simulation of heterogeneous charging infrastructures.
- **Power Transformers:** These components model the physical connection points to the grid, aggregating the electrical load from multiple chargers. They enforce the physical power limits of the local distribution network and can model inflexible base loads (e.g., buildings) and local renewable generation (e.g., solar panels).
- **Electric Vehicles (EVs):** Dynamic and autonomous agents, each defined by its battery capacity, power limits, current and desired energy levels, and specific arrival and departure times.

The simulation process follows a reproducible three-phase structure: (1) **Initialization** from a comprehensive YAML configuration file, (2) a discrete-time **Simulation Loop** where the agent interacts with the environment, and (3) a final **Evaluation and Visualization** phase that generates standardized performance metrics.

3.2 A Unified Experimentation and Evaluation Workflow

A key contribution of this thesis is the development of a unified and powerful experimentation workflow, orchestrated primarily by the `run_experiments.py` script (with an interactive interface provided by `run_interactive.py`). This approach replaces the previous fragmentation, offering a single platform to manage the entire lifecycle of training, benchmarking, and evaluation for V2G control agents. The workflow is designed to be both flexible for research and rigorous for evaluation, supporting the goal of developing both specialized and generalized agents.

3.2.1 Orchestration and Execution Interfaces

The `run_experiments.py` script serves as the central hub for all experimentation. To ensure flexibility and reproducibility, the project offers two execution modes:

1. **Interactive Mode (`run_interactive.py`):** Provides a guided, step-by-step command-line interface, ideal for initial configuration, testing, and running single experiments. The user responds to successive prompts to select scenarios, algorithms, and training parameters.
2. **Scripted/Batch Mode (`run_experiments.py`):** Utilizes the `argparse` module to accept all configuration parameters (e.g., `-scenarios`, `-reward_func`, `-training_mode`) directly as command-line arguments. This mode is essential for automation, reproducibility, and running large batches of experiments on servers or high-performance computing systems.

The key steps in the workflow include:

- **Algorithm Selection:** The script dynamically defines the algorithms to be executed, which can include Deep Reinforcement Learning agents (e.g., SAC, DDPG+PER, TQC), classical optimization methods (Model Predictive Control), and heuristics (e.g., AFAP, ALAP).
- **Scenario and Reward Selection:** The user selects one or more `.yaml` configuration files and the desired reward function from the `reward.py` module.
- **Battery Calibration:** The option to run `Fit_battery.py` is provided to calibrate the parameters of the battery degradation model, ensuring that simulations use the most up-to-date data.

3.2.2 Scenario structure Yaml file

The YAML (YAML Ain't Markup Language) configuration file serves as the foundational blueprint for defining a simulation experiment within the EV2Gym framework. It is a powerful and indispensable tool for the systematic study

of EV smart charging strategies. It provides a structured and transparent method for defining the physical, economic, and stochastic properties of the simulation environment. A thorough understanding and deliberate manipulation of these parameters are essential for formulating meaningful research questions, generating valid results, and drawing robust conclusions about the performance of various control algorithms.

3.3 Core Simulation Parameters

This primary section establishes the temporal boundaries and fundamental operational logic of the simulation.

timescale Defines the temporal granularity of a single simulation step, measured in minutes. This parameter is critical as it dictates the resolution of the control problem; a smaller timescale allows for finer control but increases computational complexity.

```
1 # Timescale in minutes per simulation step
2 timescale: 15
3
```

simulation_length Specifies the total duration of a single simulation episode, measured in the number of steps defined by `timescale`.

```
1 # Duration in steps per simulation
2 simulation_length: 112
3
```

3.4 Temporal and Contextual Settings

These parameters anchor the simulation to a specific point in time, which is crucial for sourcing external data such as electricity prices and solar irradiance profiles.

date The `year`, `month`, and `day` parameters set the initial date. The `random_day` boolean determines if a new, random date is selected upon each environment reset, facilitating stochastic analysis over different time periods.

```
1 year: 2022
2 month: 1
3 day: 17
4 random_day: True
5
```

time The initial hour and `minute` of the simulation. These typically remain fixed across resets to ensure consistent starting conditions.

simulation_days Constrains the simulation to specific day types (`weekdays`, `weekends`, or both), allowing for the study of distinct demand patterns.

3.5 Stochastic Demand Modeling

This section governs the arrival and behavior of Electric Vehicles (EVs), which constitute the primary source of flexible load in the simulation.

scenario Defines the archetypal environment (e.g., `workplace`, `public`, `private`), which loads a corresponding statistical model for EV arrival times, departure times, and required energy.

spawn_multiplier A scalar value that adjusts the baseline EV arrival rate. A value greater than 1 increases the density of EVs, thereby intensifying the stress on the charging infrastructure and creating more challenging control problems.

```
1 scenario: workplace
2 spawn_multiplier: 5
3
```

3.6 Economic Framework

These parameters establish the financial incentives and constraints that drive the optimization objective.

discharge_price_factor A foundational economic lever for Vehicle-to-Grid (V2G) operations. It defines the remuneration for discharging energy back to the grid as a fraction of the purchasing price. A value less than 1.0 models a realistic bid-ask spread, ensuring economic viability for the grid operator.

```
1 # A factor of 0.95 means selling energy yields 95% of the
  purchasing price.
2 discharge_price_factor: 0.95
3
```

3.7 Physical Infrastructure

This section specifies the hardware and topological constraints of the charging network. These are the "hard" constraints that no algorithm can violate without incurring significant penalties.

v2g_enabled A global boolean flag to enable or disable V2G capabilities for all charging stations.

number_of_charging_stations The total count of charging points available.

transformer Defines the properties of the local transformer, most critically its `max_power` capacity in kW. This parameter represents the primary bottleneck of the system; exceeding this limit results in an overload condition.

```
1 transformer:  
2   max_power: 100 # in kW  
3
```

charging_station Specifies the default electrical properties of a charging station, including maximum current, voltage, and number of phases. These are used to calculate the maximum power per station.

```
1 charging_station:  
2   max_charge_current: 32 # Amperes  
3   voltage: 400 # Volts  
4   phases: 3  
5
```

3.8 Exogenous Energy Events

These parameters introduce external, often uncontrollable, energy flows and grid requests that add realism and complexity to the simulation.

inflexible_loads Models background energy consumption from sources other than EVs (e.g., building lighting, HVAC). When enabled, this load consumes a portion of the transformer's capacity, reducing the available power for EV charging.

solar_power Simulates on-site photovoltaic generation. This introduces a source of low-cost, intermittent energy that intelligent algorithms can leverage to reduce charging costs.

demand_response Models a request from the grid operator to curtail power consumption for a specified duration. The `notification_of_event_minutes` parameter is crucial, as it provides the forecast horizon that advanced control algorithms (like MPC) require to plan and adapt their charging strategies effectively.

3.9 Electric Vehicle Fleet Specification

This section defines the characteristics of the vehicles being charged.

heterogeneous_ev_specs A boolean that, if true, populates the simulation with a diverse fleet of EVs with varying battery capacities and charging rates, as defined in the `ev_specs_file`. This enhances simulation realism.

ev This subsection defines the default properties of a single EV. Key parameters include:

- `charge_efficiency` and `discharge_efficiency`: Model the energy losses inherent in the charging and discharging processes. Values less than 1.0 are physically realistic and are the source of the `Q_lost` metric.

- `desired_capacity`: Represents the target state-of-charge requested by the user, modeling the fact that not all users require a full 100% charge.

```

1 ev:
2   charge_efficiency: 0.95
3   discharge_efficiency: 0.95
4   desired_capacity: 0.9
5

```

3.9.1 Dual-Mode Training: Specialists and Generalists

The new workflow seamlessly manages the training of both "specialist" agents (optimized for a single scenario) and "generalist" agents (robust across multiple scenarios). The behavior is determined by the number of selected scenarios:

- **Single-Domain Specialization:** If only one scenario is selected, the RL agent is trained exclusively on that EV2Gym environment.
- **Multi-Scenario Generalization:** If multiple scenarios are selected, the script automatically utilizes the custom `MultiScenarioEnv` wrapper. This Gymnasium environment:
 - **Random Selection:** At the start of each training episode, it randomly selects a configuration file and initializes a new EV2Gym environment.
 - **Handling Heterogeneous Spaces:** To allow a single neural network to control environments with a varying number of charging stations (and thus different observation and action space sizes), the maximum size (`MAX_CS`) across all scenarios is calculated. The returned observation is **padded** with zeros up to the maximum size (`max_obs_shape`), and the network's action is **sliced** to the actual size required by the current environment (`current_env.action_space.shape`). This mechanism, supported by the `CompatibilityWrapper` during evaluation, is crucial for training generalist agents.

Advanced Multi-Scenario Training Strategies

In addition to random selection, the workflow supports advanced strategies to enhance generalization:

- **Curriculum Learning (CurriculumEnv):** The agent is trained in a predefined sequence of scenarios. The environment progresses to the next curriculum level only after the agent has completed a fixed number of training steps (`steps_per_level`) in the current level. This allows for starting with simpler scenarios and progressing toward complexity.
- **Shuffled Multi-Scenario (ShuffledMultiScenarioEnv):** At the beginning of each "epoch," the list of scenarios is randomly shuffled. The agent runs one full episode on each scenario in this random order before the list is reshuffled for the next epoch. This ensures the agent sees all scenarios in a non-repetitive order within a complete cycle.

3.9.2 MPC Integration and Approximation

The workflow integrates both classical MPC and its approximations:

- **Linear MPC:** The `run_experiments.py` script utilizes an MPC based on a linear optimization model (`OnlineMPC_Solver`).
- **Approximate Explicit MPC:** The scripts `train_mpc_approximator.py` and `train_mpc_approximator_nn.py` are dedicated to creating an **Approximate Explicit MPC**. This process:
 1. Generates a dataset of samples (state, optimal action) by solving the MPC problem (the oracle) across a large number of random states in different scenarios.
 2. Trains a Machine Learning model (Random Forest in `train_mpc_approximator.py` or a Neural Network in `train_mpc_approximator_nn.py`) to map the state to the optimal action.

This approach drastically reduces runtime computation, transforming a complex optimization problem into a simple model inference, making MPC suitable for real-time control and providing a high-speed performance baseline.

3.9.3 Rigorous and Reproducible Benchmarking

The `run_benchmark` function in `run_experiments.py` is designed to ensure fair and rigorous evaluation:

- **Replay Mechanism:** To compare algorithms under identical conditions, the benchmark first runs a "replay" simulation with a null action, saving the entire sequence of stochastic events (EV arrivals, prices, etc.) to a `.pkl` file. Subsequently, each algorithm is evaluated by loading and reproducing *exactly* the same event sequence. This eliminates stochastic variability between runs, making the comparison between algorithms highly reliable.
- **Performance Metrics:** Results are aggregated over multiple simulations (`num_simulations`) and include key metrics such as:
 - Total Profit (€)
 - Average User Satisfaction (%)
 - Peak Transformer Loading (%)
 - Total Battery Degradation (%), with detail on cyclic loss and calendar loss.
- **Automatic Visualization:** Plotting functions (`plot_performance_metrics`, `plot_degradation_details`) automatically generate bar charts for the key metrics, grouping algorithms by category (heuristics, MPC, RL On-Policy, RL Off-Policy) for clear visual analysis.

3.9.4 Software Implementation and Project Structure

The practical implementation is organized within a modular Python package named `ev2gym`. This structure promotes code reusability and separation of concerns. High-level experimentation scripts, such as `run_experiments.py` and `train_mpc_approximator.py`, reside in the project's root directory and orchestrate experiments by utilizing the core functionalities provided by the `ev2gym` package.

The key subdirectories within the `ev2gym` package are:

- `baselines/`: Contains implementations for all non-RL controllers, including rule-based heuristics (in `heuristics.py`) and all variants of the Model Predictive Controllers (in `pulp_mpc.py`).
- `rl_agent/`: The central location for all Reinforcement Learning logic, containing modules for state vector construction (`state.py`), the library of available reward functions (`reward.py`), and the implementation of custom RL algorithms (`custom_algorithms.py`).
- `utilities/`: A collection of helper functions and utility classes used across the entire framework.
- `models/`: Designated for storing serialized, pre-trained machine learning models, such as the Random Forest model used by the Approximate-Explicit MPC.

This modular software design allows for independent development and testing of different components, such as control algorithms and reward functions, while maintaining a consistent and unified simulation environment.

3.10 Core Physical Models

The simulation's fidelity depends on its detailed, empirically validated models, which are necessary for developing control strategies robust enough for real-world application.

3.10.1 EV Model and Charging/Discharging Dynamics

The framework implements a realistic two-stage charging/discharging model that captures the non-linear behavior of lithium-ion batteries, simulating both the **constant current (CC)** and **constant voltage (CV)** phases. Each EV is defined by a comprehensive parameter set: maximum capacity (E_{max}), a minimum safety capacity (E_{min}), separate power limits for charging and discharging ($P_{ch}^{max}, P_{dis}^{max}$), and distinct efficiencies for each process (η_{ch}, η_{dis}).

3.10.2 Battery Degradation Model

To address the critical issue of battery health in V2G operations, the simulator incorporates a semi-empirical battery degradation model. It quantifies capacity loss (Q_{lost}) as the sum of two primary aging mechanisms [32]: calendar aging and cyclic aging.

- **Calendar Aging (d_{cal}):** Time-dependent capacity loss, influenced by the battery's average State of Charge (SoC) and temperature (Θ). The formula is:

$$d_{cal} = 0.75 \cdot (\epsilon_0 \cdot \overline{SoC} - \epsilon_1) \cdot e^{-\epsilon_2/\Theta} \cdot \frac{t_{days}}{(t_{days} + 1)^{0.25}} \quad (3.1)$$

- **Cyclic Aging (d_{cyc}):** Wear resulting from charge/discharge cycles, dependent on energy throughput ($E_{exchanged}$), depth-of-cycle (implicitly via \overline{SoC}), and the total accumulated charge (Q_{acc}). The formula is:

$$d_{cyc} = (\zeta_0 + \zeta_1 \cdot |\overline{SoC} - 0.5|) \cdot \frac{E_{exchanged}}{\sqrt{Q_{acc}}} \quad (3.2)$$

The total capacity loss is the sum $Q_{lost} = d_{cal} + d_{cyc}$. This integrated model enables direct quantification of how different control strategies impact the battery's long-term State of Health (SoH), supporting the training of agents that balance profitability with battery preservation.

A key feature of this framework is that the physical parameters for this model ($\epsilon_0, \epsilon_1, \epsilon_2, \zeta_0, \zeta_1, Q_{acc}$) are not fixed. They can be empirically calibrated from real-world experimental data using the provided `Fit_battery.py` script, as detailed in Section 3.12.

3.10.3 Reproducible Benchmarking and Evaluation

To ensure a fair and scientifically valid comparison, the `run_benchmark` function implements a rigorous evaluation protocol. For each scenario, it first generates a "replay" file containing the exact sequence of stochastic events (e.g., EV arrivals, energy demands). This exact same sequence is then used to evaluate every algorithm, eliminating randomness as a factor in performance differences. The script runs multiple simulations for statistical robustness, aggregates the mean results, and automatically generates a suite of comparative plots, including overall performance metrics and detailed battery degradation analyses.

3.10.4 Interactive Web-Based Dashboard

To complement the command-line-driven workflow, the project includes an interactive web-based dashboard built with the Streamlit library, executed via the `streamlit_app.py` script. This graphical user interface (GUI) serves two primary functions, significantly enhancing usability and accessibility for experimentation and results analysis.

Simulation Orchestrator

The first part of the dashboard acts as a GUI wrapper for the `run_experiments.py` script. It provides a user-friendly web form where users can:

- Select which algorithms to benchmark from a multi-select list.
- Choose one or more scenarios to test.
- Pick a specific reward function for the RL agents from a dropdown menu.
- Set simulation parameters, such as the number of evaluation runs.
- Toggle optional steps, like running the `Fit_battery.py` calibration or enabling RL model training.

Upon clicking the "Run Simulation" button, the application constructs the equivalent command-line arguments and executes `run_experiments.py` as a subprocess. It captures and displays the console output in real-time on the web page, providing a seamless user experience without requiring direct terminal interaction.

Results Visualizer

The second part of the dashboard is a dedicated results browser. It automatically scans the `results/` directory and presents a list of all completed benchmark runs (organized by timestamp). The user can select a specific benchmark, and the application will find and display all the generated plots (e.g., performance comparisons, battery degradation graphs) directly on the page. This feature allows for quick and convenient inspection and comparison of outcomes from different experiments.

3.11 Evaluation Metrics

To ensure a fair and comprehensive comparison, all algorithms are evaluated against an identical set of pre-generated scenarios through a "replay" mechanism. The **mean** and **standard deviation** of performance are calculated across multiple simulation runs. The key metrics include:

- **Total Profit (\$):** The net economic outcome, calculated as revenue from energy sales minus the cost of energy purchases.

$$\Pi_{\text{total}} = \sum_{t=0}^{T_{\text{sim}}} \sum_{i=1}^N (C_{\text{sell}}(t)P_{\text{dis},i}(t) - C_{\text{buy}}(t)P_{\text{ch},i}(t)) \Delta t$$

- **Tracking Error (RMSE, kW):** For grid-balancing scenarios, this measures the root-mean-square error between the fleet's aggregated power and a target setpoint.

$$E_{\text{track}} = \sqrt{\frac{1}{T_{\text{sim}}} \sum_{t=0}^{T_{\text{sim}}-1} (P_{\text{setpoint}}(t) - P_{\text{total}}(t))^2}$$

- **User Satisfaction (Average):** The fraction of energy delivered compared to what was requested by the user, averaged across all EV sessions. A score of 1 indicates perfect service.

$$US_{\text{avg}} = \frac{1}{N_{\text{EVs}}} \sum_{k=1}^{N_{\text{EVs}}} \min \left(1, \frac{E_k(t_k^{\text{dep}})}{E_k^{\text{des}}} \right)$$

- **Transformer Overload (kWh):** The total energy that exceeded the transformer's rated power limit. An ideal controller should achieve a value of 0.

$$O_{\text{tr}} = \sum_{t=0}^{T_{\text{sim}}} \sum_{j=1}^{N_T} \max(0, P_j^{\text{tr}}(t) - P_j^{\text{tr,max}}) \cdot \Delta t$$

- **Battery Degradation (\$):** The estimated monetary cost of battery aging due to both cyclic and calendar effects.

$$D_{\text{batt}} = \sum_{k=1}^{N_{\text{EVs}}} (\text{CyclicCost}_k + \text{CalendarCost}_k)$$

3.12 Simulator Implementation Details

During the analysis and implementation of new metrics, fundamental details about the EV2Gym simulator's architecture emerged, which warrant documentation. The configuration of Electric Vehicles (EVs) and the calculation of their degradation follow a specific logic dependent on a key parameter in the .yaml configuration files.

Vehicle Definition Modes

The simulator operates in two distinct modes, controlled by the boolean flag `heterogeneous_ev_specs`:

- **Heterogeneous Mode (True):** In this mode, the simulator ignores the default vehicle specifications in the .yaml file. Instead, it loads a list of vehicle profiles from an external JSON file, specified by the `ev_specs_file` parameter (e.g., `ev_specs_v2g_enabled2024.json`). This allows for the creation of a realistic fleet with diverse battery capacities, charging powers, and efficiencies. For instance, the fleet may include a **Peugeot 208** with a 46.3 kWh battery and a 7.4 kW charge rate, alongside a **Volkswagen ID.4** with a 77 kWh battery and an 11 kW charge rate. A vehicle is randomly selected from this list for each new arrival event.

- **Homogeneous Mode (False):** In this mode, the external JSON file is ignored. All vehicles created in the simulation are identical, and their characteristics are defined exclusively by the `ev:` block within the `.yaml` configuration file. The `battery_capacity` parameter in this block becomes the single source of truth for the entire fleet.

Empirical Calibration of the Degradation Model

A significant enhancement in this work is the move towards a more physically representative and flexible battery degradation model. While the underlying semi-empirical model for calendar and cyclic aging remains, the methodology for parameterizing it has been fundamentally improved, addressing previous inconsistencies. This is achieved through the `Fit_battery.py` script, a new utility for empirical model calibration. The script implements the following workflow:

1. **Data Loading:** It loads time-series data from real-world battery aging experiments. The expected data includes measurements of capacity loss over time, along with contextual variables like state of charge (SoC), temperature, and energy throughput.
2. **Model Fitting:** Using the `curve_fit` function from the SciPy library, the script fits the parameters of the `Qlost_model` (which combines calendar and cyclic aging) to the empirical data. This optimization process finds the physical constants (e.g., ϵ_0 , ζ_0) that best explain the observed degradation.
3. **Parameter Export:** The script outputs the calibrated parameters. These values can then be used directly in the simulator's configuration, ensuring that the degradation model for a specific EV fleet is grounded in experimental evidence for that battery type.

This calibration workflow, integrated optionally into the main `run_experiments.py` script, elevates the simulation's fidelity. It allows the framework to move beyond a single, fixed degradation model (previously calibrated for a 78 kWh battery) and enables the creation of high-fidelity digital twins for a wide variety of EV batteries, provided that the necessary experimental data is available.

3.13 Simulation Framework Components

The simulation environment is constructed from a set of modular classes, each representing a key physical or logical component of the EV charging ecosystem. This section details the implementation and mathematical underpinnings of each component.

3.13.1 Electric Vehicle Model (`ev.py`)

The EV class is the most fundamental component, encapsulating the state, physical constraints, and charging behavior of a single electric vehicle. It serves as the primary dynamic element within the simulation.

State and Attribute Representation

Each EV instance is defined by a set of static and dynamic attributes that govern its behavior throughout its connection period.

- **Static Attributes:** These are defined upon the EV's arrival and remain constant. They include the maximum battery capacity (E_i^{\max}), a minimum operational capacity (E_i^{\min}), maximum AC charging power ($P_i^{\text{ch},\max}$), maximum discharging power ($P_i^{\text{dis},\max}$), charging efficiency (η_{ch}), discharging efficiency (η_{dis}), arrival time (t_i^{arr}), and departure time (t_i^{dep}).
- **Dynamic State Variables:** The core state variable is the current energy stored in the battery, denoted as $E_{i,t}$ at time step t . This state is updated at every simulation step.
- **Goal-Oriented Attributes:** The EV's objective is defined by its desired energy at departure, E_i^{des} . This is used to calculate user satisfaction.

Charging and Discharging Dynamics

The model implements a sophisticated two-stage charging process to accurately reflect the behavior of lithium-ion batteries, particularly the transition from the constant current (CC) to the constant voltage (CV) phase.

Two-Stage Charging Model (_charge method). The charging rate is not constant up to full capacity. The model captures the characteristic tapering of current as the battery approaches its maximum charge.

1. **Constant Current (CC) Phase:** When the State of Charge ($SoC_{i,t}$) is below a transition threshold, SoC^{trans} , the battery charges at a constant power. The rate of change of energy is limited by both the pilot signal from the charger, $P_{i,t}^{\text{pilot}}$, and the EV's own maximum charging power, $P_i^{\text{ch},\max}$. The effective charging power is $P_{i,t}^{\text{ch}} = \min(P_{i,t}^{\text{pilot}}, P_i^{\text{ch},\max})$. The energy evolution is:

$$E_{i,t} = E_{i,t-1} + \eta_{\text{ch}} \cdot P_{i,t}^{\text{ch}} \cdot \frac{\Delta t}{60} \quad (3.3)$$

where Δt is the timescale in minutes.

2. **Constant Voltage (CV) Phase:** Once $SoC_{i,t}$ exceeds SoC^{trans} , the charging power begins to decrease, even if the pilot signal remains high. The implementation in the _charge method approximates this tapering effect using an exponential decay function. The model calculates a new transition SoC based on the pilot signal and then computes the new SoC using a formula that ensures a smooth, decaying charge rate as the SoC approaches 100%. This prevents unrealistic assumptions of constant maximum power charging until the battery is full.

Discharging Model (_discharge method). Discharging is modeled as a linear process, constrained by the EV's maximum discharge power and the battery's minimum energy level. The energy delivered to the grid, $P_{i,t}^{\text{dis}}$, results in a larger energy withdrawal from the battery due to inefficiency:

$$E_{i,t} = E_{i,t-1} + \frac{P_{i,t}^{\text{dis}}}{\eta_{\text{dis}}} \cdot \frac{\Delta t}{60} \quad (3.4)$$

where $P_{i,t}^{\text{dis}}$ is negative by convention. The operation is constrained such that $E_{i,t} \geq E_i^{\min}$.

User Satisfaction Metric

Upon departure at time t_i^{dep} , the performance of the charging service is quantified by a user satisfaction metric, S_i . This is defined as the ratio of the final energy level to the desired energy level, capped at 100%.

$$S_i = \min \left(1, \frac{E_{i,t_i^{\text{dep}}}}{E_i^{\text{des}}} \right) \quad (3.5)$$

This metric provides a crucial feedback signal for control algorithms, penalizing strategies that fail to meet user requirements.

3.13.2 Charging Station Model (`ev_charger.py`)

The EV_Charger class acts as an intermediary between the grid infrastructure and the individual EVs. It manages a collection of charging ports and enforces its own set of physical and operational constraints.

Role and Attributes

A charging station (CS) is defined by its number of ports (N_{ports}), its maximum aggregate charging and discharging currents ($I_{\text{CS}}^{\max,\text{ch}}, I_{\text{CS}}^{\max,\text{dis}}$), its operating voltage (V), and the number of phases. It serves as a local aggregation point for power and energy.

Operational Logic (step method)

At each simulation step, the `step` method executes the core logic of the charging station:

1. **Action Translation:** It receives a normalized action vector $a_t \in [-1, 1]^{N_{\text{ports}}}$. For each port j , it translates the normalized action $a_{j,t}$ into a physical pilot current signal, $I_{j,t}^{\text{pilot}}$.

$$I_{j,t}^{\text{pilot}} = \begin{cases} a_{j,t} \cdot I_{\text{CS}}^{\max,\text{ch}} & \text{if } a_{j,t} > 0 \\ a_{j,t} \cdot |I_{\text{CS}}^{\max,\text{dis}}| & \text{if } a_{j,t} < 0 \\ 0 & \text{if } a_{j,t} = 0 \end{cases} \quad (3.6)$$

2. **EV Interaction:** It passes this pilot current to the `step` method of the corresponding connected EV instance, which then calculates its actual power exchange based on its internal two-stage model.
3. **Power Aggregation:** It aggregates the actual power, $P_{j,t}$, from all its ports to determine its total power exchange with the grid at that time step.

$$P_{CS,t} = \sum_{j=1}^{N_{\text{ports}}} P_{j,t} \quad (3.7)$$

4. **Economic Calculation:** It calculates the net profit for the time step based on the aggregated energy and real-time electricity prices ($c_t^{\text{buy}}, c_t^{\text{sell}}$).
5. **Departure Management:** It checks for departing EVs, collects their final user satisfaction scores, and frees up the corresponding ports.

3.13.3 Transformer Model (`transformer.py`)

The `Transformer` class represents a critical piece of grid infrastructure, modeling the point of common coupling for a group of charging stations and other local loads. Its primary function is to enforce an aggregate power limit.

Model Components

Each transformer is characterized by its maximum power capacity, P_{TR}^{\max} . It also manages two external time-series data streams:

- **Inflexible Load (P_t^{inflex}):** Represents the background power consumption from other sources (e.g., buildings) connected to the same transformer.
- **Solar Power (P_t^{PV}):** Represents local photovoltaic generation, which acts as a negative load.

Core Functionality

The transformer's logic is centered around monitoring its total load and checking for capacity violations.

Load Aggregation. At each time step t , the total power flowing through the transformer, $P_{\text{TR},t}$, is the algebraic sum of the inflexible load, the solar generation, and the sum of the power from all charging stations connected to it.

$$P_{\text{TR},t} = P_t^{\text{inflex}} + P_t^{\text{PV}} + \sum_{i \in \text{CSs connected to TR}} P_{\text{CS},i,t} \quad (3.8)$$

Overload Detection. The critical function is `is_overloaded`, which returns true if the absolute total power exceeds the transformer's rating. This condition serves as a primary constraint for the control problem.

$$\text{Overload} \iff |P_{\text{TR},t}| > P_{\text{TR}}^{\max} \quad (3.9)$$

Forecasting with Uncertainty. The model includes methods (`generate_..._forecast`) to simulate imperfect knowledge of future loads and generation. It creates forecasts by taking the true profiles and adding zero-mean Gaussian noise, where the standard deviation is a configurable percentage of the true value. This allows for the development of robust control strategies that can handle prediction errors.

3.13.4 Main Gym Environment (`ev2gym_env.py`)

The `EV2Gym` class is the central orchestrator of the entire simulation. It integrates all the aforementioned physical models into a cohesive whole and exposes it through the standardized `gymnasium.Env` interface, making it compatible with a wide range of reinforcement learning algorithms.

Environment Structure and Main Loop

The class manages the high-level simulation flow.

Initialization (`__init__`). Upon creation, the environment reads a configuration file to instantiate all the necessary components: it creates the specified number of `Transformer` and `EV_Charger` objects, loads the EV arrival scenarios, and sets up electricity price profiles.

Simulation Step (`step(actions)`). This method drives the simulation forward by one time step (Δt). The sequence of operations is as follows:

1. It receives a single, flat action vector containing the control signals for every charging port in the entire system.
2. It slices this vector and passes the appropriate actions to each `EV_Charger`'s `step` method.
3. This triggers the `step` methods of all connected EVs, updating their internal states ($E_{i,t}$).
4. It aggregates the resulting power at each `Transformer` and checks for overload conditions.
5. It processes the EV queue, spawning new EVs that are scheduled to arrive at the next time step.
6. It computes a scalar reward signal using a user-defined reward function.

7. It constructs the next state observation using a user-defined state representation function.
8. It checks for termination conditions (e.g., simulation end, constraint violation).
9. It returns the standard '(observation, reward, terminated, truncated, info)' tuple.

Reset (reset). This method re-initializes the entire environment to a starting state, allowing for the start of a new simulation episode, which could represent a new day or a different random scenario.

3.14 Reinforcement Learning Formulation

The control problem is formalized as a Markov Decision Process (MDP), defined by the tuple (S, A, P, R, γ) .

3.14.1 State Space (S)

The state $s_t \in S$ is a feature vector providing a comprehensive snapshot of the environment at time t . The composition of this vector is crucial for the agent's performance, as it encapsulates all the information available for decision-making. The framework is designed to be flexible, allowing different state representations to be defined in the `ev2gym/r1_agent/state.py` module. For the primary task of profit maximization under grid constraints, the `V2G_profit_max_loads` function is used.

The process of constructing this state vector at each timestep is formally described in Algorithm 1. It involves gathering temporal, historical, predictive, and physical information from the environment.

Algorithm 1 State Vector Construction (V2G_profit_max_loads)

```

1: function BUILDSTATEVECTOR(environment env)
2:   Initialize: Empty state list  $S_{list} \leftarrow \emptyset$ .
3:   ▶ 1. Add temporal and historical information
4:   Append current timestep  $env.current\_step$  to  $S_{list}$ .
5:   Append total power from previous step  $env.current\_power\_usage[t - 1]$ 
   to  $S_{list}$ .
6:   ▶ 2. Add predictive market information
7:   Get future charge prices for horizon  $H$ :  $\mathbf{c} \leftarrow env.charge\_prices[t : t + H]$ .
8:   Pad  $\mathbf{c}$  with the last known value if horizon extends beyond simulation end.
9:   Append  $\mathbf{c}$  to  $S_{list}$ .
10:  ▶ 3. Add predictive physical constraints and loads for each transformer
11:  for each transformer  $tr$  in  $env.transformers$  do
12:    Get forecasts for horizon  $H$ :  $\mathbf{L}, \mathbf{PV} \leftarrow tr.get\_load\_pv\_forecast(t, H)$ .
13:    Get future power limits for horizon  $H$ :  $\mathbf{P}_{lim} \leftarrow tr.get\_power\_limits(t, H)$ .
14:    Append net load forecast ( $\mathbf{L} - \mathbf{PV}$ ) to  $S_{list}$ .
15:    Append power limits  $\mathbf{P}_{lim}$  to  $S_{list}$ .
16:    ▶ 4. Add information for each connected EV
17:    for each charging station  $cs$  connected to  $tr$  do
18:      for each EV slot in  $cs$  do
19:        if an EV is connected then
20:           $SoC \leftarrow EV.get\_soc()$ .
21:           $t_{rem} \leftarrow EV.time\_of\_departure - env.current\_step$ .
22:          Append  $[SoC, t_{rem}]$  to  $S_{list}$ .
23:        else
24:          Append  $[0, 0]$  to  $S_{list}$  for padding.
25:        end if
26:      end for
27:    end for
28:  end for
29:  return Flatten( $S_{list}$ ) into a single vector  $s_t$ .
30: end function

```

The resulting state vector s_t is a concatenation of these components, forming a high-dimensional representation suitable for a deep neural network policy. Mathematically, it can be expressed as:

$$s_t = [t, P_{total}(t - 1), \mathbf{c}(t, H), \mathbf{NL}_1(t, H), \mathbf{P}_1^{lim}(t, H), \dots, \mathbf{s}_1^{EV}(t), \dots, \mathbf{s}_N^{EV}(t)]^T$$

where the components are:

- t : The current time step, providing temporal context.
- $P_{total}(t - 1)$: The aggregated power from the previous time step, serving as a feedback signal of the last action's outcome.

- $\mathbf{c}(t, H)$: A vector of **predicted future** electricity prices over a horizon H (e.g., 20 steps).
- $\mathbf{NL}_j(t, H), \mathbf{P}_j^{\text{lim}}(t, H)$: Forecasts for the net inflexible loads (loads minus solar generation) and the power limits for each transformer j .
- $\mathbf{s}_i^{\text{EV}}(t) = [\text{SoC}_i(t), t_i^{\text{rem}}]$: A sub-vector containing the most critical information for each EV i : its current State of Charge and its remaining time until departure ($t_i^{\text{dep}} - t$). If a charger is empty, this sub-vector is padded with zeros to maintain a fixed state size.

This state representation is deliberately rich, providing the agent with a multi-faceted view of the system. It combines temporal awareness, feedback from past actions, predictive information about market conditions and physical constraints, and the specific needs of each vehicle. This comprehensive view is essential for enabling the agent to learn sophisticated, forward-looking policies that can effectively balance immediate profit opportunities with long-term obligations to users and the grid.

3.14.2 Action Space (A)

The action $a_t \in A$ is a continuous vector in \mathbb{R}^N , where N is the number of chargers. For each charger i , the command $a_i(t) \in [-1, 1]$ is a normalized value that is translated into a power command:

- If $a_i(t) > 0$, the EV is charging: $P_i(t) = a_i(t) \cdot P_{\text{charge},i}^{\max}$.
- If $a_i(t) < 0$, the EV is discharging (V2G): $P_i(t) = a_i(t) \cdot P_{\text{discharge},i}^{\max}$.

3.14.3 Reward Function (R)

The reward function $R(t)$ encodes the objectives of the control agent. The framework allows for the selection of different reward functions from the `reward.py` module to suit various goals.

3.15 Reinforcement Learning Algorithms

This work benchmarks several state-of-the-art Deep Reinforcement Learning algorithms. The following sections provide a detailed mathematical description of the selected off-policy, actor-critic algorithms that form the core of the experimental comparison.

Soft Actor-Critic (SAC)

SAC is an off-policy actor-critic algorithm designed for continuous action spaces that optimizes a stochastic policy. Its distinguishing feature is the explicit incorporation of entropy maximization into the objective function, which promotes

exploration and yields policies that are more robust to model inaccuracies and environmental perturbations. Unlike traditional RL algorithms that focus solely on reward maximization, SAC aims to maximize both the expected cumulative reward and the entropy of the policy distribution.

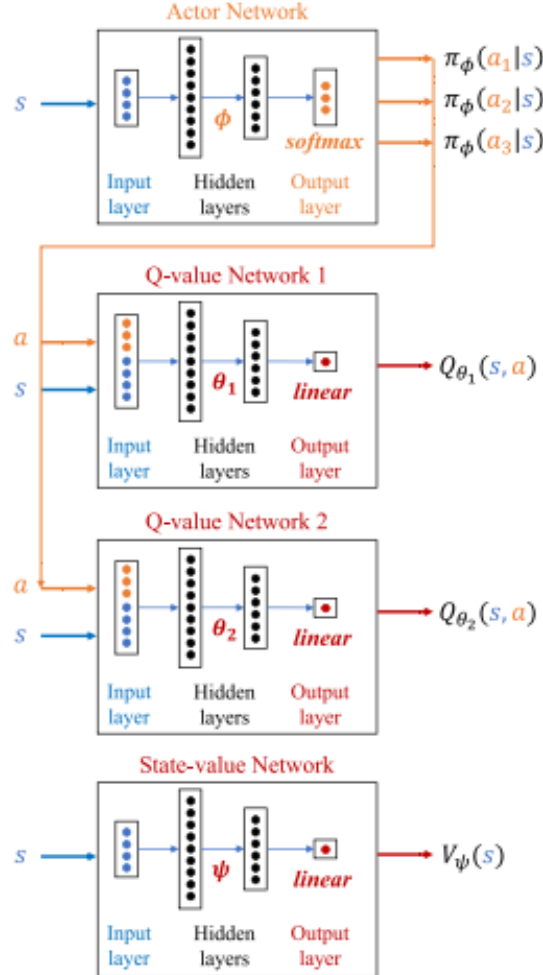


Figure 3.2: SAC actor-critic architecture. The actor network outputs a stochastic policy parameterized by a mean and standard deviation, while two separate Q-networks (critics) estimate state-action values. The minimum of the two Q-values is used for policy updates to mitigate overestimation bias. Image from [35].

The objective function is:

$$J(\pi) = \sum_{t=0}^T \mathbb{E}_{(s_t, a_t) \sim \rho_\pi} [r(s_t, a_t) + \alpha \mathcal{H}(\pi(\cdot|s_t))]$$

where \mathcal{H} is the entropy of the policy π , defined as $\mathcal{H}(\pi(\cdot|s_t)) = -\mathbb{E}_{a_t \sim \pi} [\log \pi(a_t|s_t)]$, and α is the temperature parameter, which controls the trade-off between reward exploitation and entropy-driven exploration. A higher α encourages more stochastic behavior, while a lower α biases the policy toward deterministic, reward-

maximizing actions. The complete training procedure is outlined in Algorithm 2.

Algorithm 2 Soft Actor-Critic (SAC)

```

1: Initialize critic networks  $Q_{\theta_1}, Q_{\theta_2}$  and actor network  $\pi_\phi$  with random parameters.
2: Initialize target networks  $\bar{\theta}_1 \leftarrow \theta_1, \bar{\theta}_2 \leftarrow \theta_2$ .
3: Initialize replay buffer  $D$ .
4: Initialize temperature parameter  $\alpha$ .
5: for each timestep  $t = 1, \dots, T$  do
6:   Select action with exploration:  $a_t \sim \pi_\phi(\cdot|s_t)$ .
7:   Execute action  $a_t$  and observe reward  $r_t$  and next state  $s_{t+1}$ .
8:   Store transition  $(s_t, a_t, r_t, s_{t+1})$  in replay buffer  $D$ .
9:   if  $t$  is a multiple of update frequency then
10:    Sample a minibatch of  $N$  transitions  $\{(s_j, a_j, r_j, s_{j+1})\}_{j=1}^N$  from  $D$ .
11:    ▷ Compute the target for the Q-functions
12:    With next actions  $\tilde{a}_{j+1} \sim \pi_\phi(\cdot|s_{j+1})$ :
13:     $y_j \leftarrow r_j + \gamma (\min_{i=1,2} Q_{\bar{\theta}_i}(s_{j+1}, \tilde{a}_{j+1}) - \alpha \log \pi_\phi(\tilde{a}_{j+1}|s_{j+1}))$ 
14:    ▷ Update the critic networks
15:    Update critic parameters  $\theta_i$  by one step of gradient descent on:
16:     $L(\theta_i) = \frac{1}{N} \sum_{j=1}^N (Q_{\theta_i}(s_j, a_j) - y_j)^2$  for  $i = 1, 2$ .
17:    ▷ Update the actor network
18:    With new actions  $\tilde{a}_j \sim \pi_\phi(\cdot|s_j)$ :
19:    Update policy parameters  $\phi$  by one step of gradient ascent on:
20:     $J(\phi) = \frac{1}{N} \sum_{j=1}^N (\min_{i=1,2} Q_{\theta_i}(s_j, \tilde{a}_j) - \alpha \log \pi_\phi(\tilde{a}_j|s_j))$ .
21:    ▷ Update the temperature parameter (optional)
22:    Update  $\alpha$  by one step of gradient descent on:
23:     $J(\alpha) = \frac{1}{N} \sum_{j=1}^N (-\alpha(\log \pi_\phi(\tilde{a}_j|s_j) + \bar{\mathcal{H}}))$ , where  $\bar{\mathcal{H}}$  is a target entropy.
24:    ▷ Update the target networks
25:     $\bar{\theta}_i \leftarrow \tau \theta_i + (1 - \tau) \bar{\theta}_i$  for  $i = 1, 2$ .
26: end if
27: end for

```

Implementation Details The implementation of SAC is built upon the robust, industry-standard **Stable-Baselines3** library, which provides a highly optimized and well-tested version of the algorithm. The standard SAC class from this library is used directly, leveraging its PyTorch-based backend for efficient training and inference.

SAC employs a soft Q-function, which incorporates the policy entropy into the value estimation. The soft Q-function is trained to minimize the soft Bellman residual:

$$L(\theta_Q) = \mathbb{E}_{(s_t, a_t, r_t, s_{t+1}) \sim D} \left[\left(Q(s_t, a_t) - (r_t + \gamma V_{\bar{\psi}}(s_{t+1})) \right)^2 \right]$$

where D is the replay buffer, γ is the discount factor, and the soft state value

function V is defined as:

$$V_{\text{soft}}(s_t) = \mathbb{E}_{a_t \sim \pi}[Q_{\text{soft}}(s_t, a_t) - \alpha \log \pi(a_t | s_t)]$$

To mitigate the positive bias inherent in Q-learning, SAC employs two independent Q-networks (implementing the Clipped Double-Q technique) and uses the minimum of the two target Q-values during the Bellman update. This conservative approach prevents overestimation from propagating through the learning process. Additionally, SAC can automatically tune the temperature parameter α during training by treating it as a constrained optimization problem, ensuring that the policy entropy remains above a target threshold.

Deep Deterministic Policy Gradient + PER (DDPG+PER)

DDPG is an off-policy algorithm that concurrently learns a deterministic policy $\mu(s|\theta^\mu)$ and a Q-function $Q(s, a|\theta^Q)$. It extends the Deterministic Policy Gradient (DPG) theorem to deep neural networks, enabling continuous control in high-dimensional state spaces. Unlike stochastic policy methods, DDPG directly outputs a single action for each state, which can be advantageous in environments where deterministic behavior is preferred or when the action space is high-dimensional. The full procedure, enhanced with PER, is detailed in Algorithm 3.

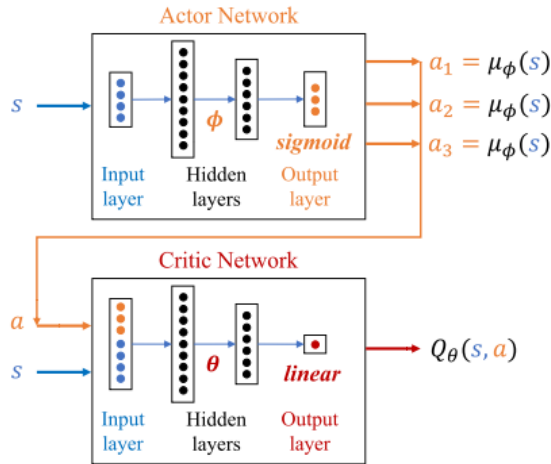


Figure 3.3: DDPG actor-critic architecture. The actor network produces a deterministic action, which is evaluated by the Q-network (critic). Both networks maintain slowly-updating target networks (μ' and Q') for stable Bellman updates. During training, exploration noise is added to the actor's output. Image from [35].

Algorithm 3 DDPG with Prioritized Experience Replay (PER)

```

1: Initialize critic network  $Q(s, a | \theta^Q)$  and actor network  $\mu(s | \theta^\mu)$  with random
   parameters.
2: Initialize target networks  $Q' \leftarrow Q$ ,  $\mu' \leftarrow \mu$ .
3: Initialize Prioritized Replay Buffer  $D$  with parameters  $\alpha, \beta$ .
4: for each episode do
5:   Initialize a random process  $\mathcal{N}$  for action exploration.
6:   Receive initial state  $s_1$ .
7:   for each timestep  $t = 1, \dots, T$  do
8:     Select action:  $a_t = \mu(s_t | \theta^\mu) + \mathcal{N}_t$ .
9:     Execute action  $a_t$  and observe reward  $r_t$  and next state  $s_{t+1}$ .
10:    Store transition  $(s_t, a_t, r_t, s_{t+1})$  in  $D$  with maximal priority.
11:    ▷ Sample from buffer and update
12:    Sample minibatch of  $N$  transitions  $\{(s_j, a_j, r_j, s_{j+1})\}_{j=1}^N$  from  $D$  with
      probabilities  $P(j) = \frac{p_j^\alpha}{\sum_k p_k^\alpha}$ .
13:    Compute importance-sampling (IS) weights  $w_j = (N \cdot P(j))^{-\beta}$ .
14:    ▷ Update the critic network
15:    Compute targets:  $y_j = r_j + \gamma Q'(s_{j+1}, \mu'(s_{j+1} | \theta^{\mu'}) | \theta^{Q'})$ .
16:    Compute TD-errors:  $\delta_j = y_j - Q(s_j, a_j | \theta^Q)$ .
17:    Update critic by minimizing the weighted loss:  $L(\theta^Q) = \frac{1}{N} \sum_{j=1}^N w_j \cdot \delta_j^2$ .
18:    Update transition priorities in  $D$ :  $p_j \leftarrow |\delta_j|$ .
19:    ▷ Update the actor network
20:    Update actor using the sampled policy gradient:
21:     $\nabla_{\theta^\mu} J \approx \frac{1}{N} \sum_{j=1}^N \nabla_a Q(s, a | \theta^Q)|_{s=s_j, a=\mu(s_j)} \nabla_{\theta^\mu} \mu(s_j | \theta^\mu)$ .
22:    ▷ Update the target networks
23:     $\theta^{Q'} \leftarrow \tau \theta^Q + (1 - \tau) \theta^{Q'}$ .
24:     $\theta^{\mu'} \leftarrow \tau \theta^\mu + (1 - \tau) \theta^{\mu'}$ .
25: end for
26: end for

```

- **Critic Update:** The critic is updated by minimizing the mean-squared Bellman error, analogous to Q-learning. Target networks (Q' and μ') are used to stabilize training by providing consistent targets during the temporal difference update.

$$L(\theta^Q) = \mathbb{E}_{(s_t, a_t, r_t, s_{t+1}) \sim D} [(y_t - Q(s_t, a_t | \theta^Q))^2]$$

where the target y_t is given by:

$$y_t = r_t + \gamma Q'(s_{t+1}, \mu'(s_{t+1} | \theta^{\mu'}) | \theta^{Q'})$$

The target networks are updated via soft updates (polyak averaging): $\theta' \leftarrow \tau \theta + (1 - \tau) \theta'$, where $\tau \ll 1$ is a small constant.

- **Actor Update:** The actor is updated using the deterministic policy gradient theorem, which states that the gradient of the expected return with respect

to the policy parameters can be computed as:

$$\nabla_{\theta^\mu} J \approx \mathbb{E}_{s_t \sim D} [\nabla_a Q(s, a | \theta^Q)|_{s=s_t, a=\mu(s_t)} \nabla_{\theta^\mu} \mu(s_t | \theta^\mu)]$$

This gradient ascent step improves the policy by moving it in the direction that increases the Q-value according to the critic's estimate.

- **Prioritized Experience Replay (PER):** This work enhances DDPG with PER, which addresses a fundamental limitation of uniform experience replay. Instead of sampling transitions uniformly from the replay buffer D , PER samples transitions according to their temporal-difference (TD) error, prioritizing experiences where the model's predictions are most inaccurate and therefore most informative. The probability of sampling transition i is:

$$P(i) = \frac{p_i^\beta}{\sum_k p_k^\beta}$$

where $p_i = |\delta_i| + \epsilon$ is the priority based on the TD-error $\delta_i = y_t - Q(s_t, a_t)$, ϵ is a small constant to ensure non-zero probabilities, and β controls the degree of prioritization. To correct for the bias introduced by non-uniform sampling, PER applies importance-sampling (IS) weights during the gradient update:

$$w_i = \left(\frac{1}{N \cdot P(i)} \right)^\alpha$$

where α controls the amount of bias correction. These weights ensure that the gradient estimator remains unbiased despite the non-uniform sampling distribution.

Implementation Details To integrate Prioritized Experience Replay (PER) with DDPG, a custom class, `CustomDDPG`, was developed in the `ev2gym/r1_agent/custom_algorithms.py` module. This class inherits from the standard DDPG agent provided by **Stable-Baselines3**. The core `train` method is overridden to replace the default uniform-sampling replay buffer with one that supports prioritized sampling. This involves calculating TD-errors for each transition, updating their priorities in the buffer, and using the resulting importance-sampling weights during the critic update, thereby focusing the learning process on the most informative experiences.

Truncated Quantile Critics (TQC)

TQC represents a significant advancement over standard SAC by modeling the entire distribution of returns rather than just its expected value. This distributional perspective, combined with a novel truncation mechanism, provides superior protection against Q-value overestimation—a persistent pathology in off-policy RL that can lead to catastrophic policy degradation. The algorithm's logic is summarized in Algorithm 4.

Algorithm 4 Truncated Quantile Critics (TQC)

- 1: Initialize critic ensemble $\{Q_{\theta_i}\}_{i=1}^N$ and actor π_ϕ with random parameters.
- 2: Initialize target networks $\{\bar{\theta}_i \leftarrow \theta_i\}_{i=1}^N$ and $\bar{\phi} \leftarrow \phi$.
- 3: Initialize replay buffer D .
- 4: Set number of quantiles N and number of quantiles to drop k .
- 5: Define quantile fractions $\tau_i = \frac{i-0.5}{N}$ for $i = 1, \dots, N$.
- 6: **for** each timestep $t = 1, \dots, T$ **do**
- 7: Select action with exploration: $a_t \sim \pi_\phi(\cdot|s_t)$.
- 8: Execute action a_t and observe reward r_t and next state s_{t+1} .
- 9: Store transition (s_t, a_t, r_t, s_{t+1}) in replay buffer D .
- 10: **if** t is a multiple of update frequency **then**
- 11: Sample a minibatch of M transitions $\{(s_j, a_j, r_j, s_{j+1})\}_{j=1}^M$ from D .
 ▷ Compute the distributional target
- 13: Sample next actions from target policy: $\tilde{a}_{j+1} \sim \pi_{\bar{\phi}}(\cdot|s_{j+1})$.
- 14: Get next-state quantile estimates from target critics: $\{Q_{\bar{\theta}_l}(s_{j+1}, \tilde{a}_{j+1})\}_{l=1}^N$.
- 15: Sort the estimates and drop the top k : $\{Q_{\text{sorted}}\}_{l=1}^{N-k}$.
- 16: Form the target quantiles: $y_{j,l} = r_j + \gamma Q_{\text{sorted},l}$ for $l = 1, \dots, N - k$.
 ▷ Update the critic networks
- 17: Update each critic θ_i by minimizing the sum of quantile Huber losses:
$$L(\theta_i) = \frac{1}{M(N-k)} \sum_{j=1}^M \sum_{l=1}^{N-k} L_{QH}^{\tau_i}(y_{j,l} - Q_{\theta_i}(s_j, a_j)).$$

 ▷ Update the actor network
- 18: Update policy ϕ by gradient ascent on:
- 19:
$$J(\phi) = \frac{1}{M} \sum_{j=1}^M \left(\frac{1}{N} \sum_{i=1}^N Q_{\theta_i}(s_j, \tilde{a}_j) - \alpha \log \pi_\phi(\tilde{a}_j|s_j) \right),$$
 where $\tilde{a}_j \sim \pi_\phi(\cdot|s_j)$.
 ▷ Update the target networks
- 20:
$$\bar{\theta}_i \leftarrow \tau \theta_i + (1 - \tau) \bar{\theta}_i$$
 for $i = 1, \dots, N$.
- 21:
$$\bar{\phi} \leftarrow \tau \phi + (1 - \tau) \bar{\phi}$$
.
- 22: **end if**
- 23: **end for**

- **Distributional Learning:** TQC employs an ensemble of N critic networks, $\{Q_{\phi_i}(s, a)\}_{i=1}^N$, where each network is trained to estimate a specific quantile τ_i of the return distribution. The target quantiles are implicitly defined as $\tau_i = \frac{i-0.5}{N}$, uniformly covering the cumulative distribution function. The critics are trained by minimizing the quantile Huber loss, L_{QH} , which is a robust asymmetric loss function that penalizes overestimation and underestimation differently:

$$L_{QH}(\delta) = |\tau_i - \mathbb{I}_{\{\delta < 0\}}| \cdot L_\kappa(\delta)$$

where L_κ is the Huber loss with threshold κ , and δ is the temporal difference error.

- **Distributional Target Calculation:** A distributional target is constructed for the Bellman update. First, an action is sampled from the target policy for the next state: $\tilde{a}_{t+1} \sim \pi_{\theta'}(\cdot|s_{t+1})$. Then, a set of N Q-value estimates for the

next state is obtained from the N target critic networks: $\{Q_{\phi'_j}(s_{t+1}, \tilde{a}_{t+1})\}_{j=1}^N$. This ensemble provides a rich representation of the value distribution's uncertainty.

- **Truncation:** This is the central innovation of TQC. To combat overestimation, the algorithm discards the k largest Q-value estimates from the set of N target values. This truncation removes the most optimistic (and typically most biased) estimates, which are the primary drivers of overestimation in ensemble methods. By dropping these outliers, TQC obtains more conservative and stable target values. The remaining $(N - k)$ quantile estimates are then used to compute the Bellman target, effectively implementing a form of pessimism that counteracts the inherent optimism bias in temporal-difference learning.
- **Critic Update:** The target value for updating the i -th critic is formed using the Bellman equation with the truncated set of next-state Q-values. The overall critic loss is the sum of the quantile losses across all critics:

$$L(\phi) = \sum_{i=1}^N \mathbb{E}_{(s,a,r,s') \sim D} [L_{QH}(r + \gamma Q_{\text{trunc}}(s', \tilde{a}') - Q_{\phi_i}(s, a))]$$

where Q_{trunc} represents the value derived from the truncated set of target quantiles. The actor is then updated using the mean of all (non-truncated) critic estimates, similar to standard SAC, but benefiting from the improved stability of the distributional value estimates.

Implementation Details The TQC algorithm is leveraged from the **SB3-Contrib** library, a collection of community-contributed extensions to Stable-Baselines3. Using the library's standard TQC implementation allows the framework to benefit from this state-of-the-art distributional RL algorithm without requiring a custom implementation from scratch. The implementation maintains the entropy-regularized objective of SAC while incorporating the distributional critics and truncation mechanism that define TQC's superior performance characteristics.

3.15.1 A History-Based Adaptive Reward for Profit Maximization

To guide the learning agent towards policies that are both highly profitable and operationally reliable, we designed a novel, history-based adaptive reward function, named `FastProfitAdaptiveReward`. This function departs from traditional approaches that use static weights for penalties. Instead, it introduces a dynamic feedback mechanism where the severity of penalties responds directly to the agent's recent performance. The core principle is to aggressively prioritize economic profit, while employing adaptive penalties as guardrails that tighten only when the agent begins to systematically violate operational constraints.

The total reward at each timestep t , R_t , is formulated as the net economic profit Π_t minus any active penalties for user dissatisfaction P_t^{sat} or transformer overload P_t^{tr} .

$$R_t = \Pi_t - P_t^{\text{sat}} - P_t^{\text{tr}} \quad (3.10)$$

The complete logic for this calculation at each timestep is detailed in Algorithm 5. The components of this reward function are defined as follows:

Π_t is the net economic profit at timestep t .

P_t^{sat} is the adaptive penalty for user dissatisfaction at timestep t .

P_t^{tr} is the adaptive penalty for transformer overload at timestep t .

\bar{S}_{hist} is the average user satisfaction score over a recent history window (e.g., 100 timesteps).

$F_{\text{hist}}^{\text{tr}}$ is the frequency of transformer overload events over a recent history window.

λ_t^{sat} and λ_t^{tr} are the dynamically computed severity multipliers for the satisfaction and overload penalties, respectively.

Algorithm 5 History-Based Adaptive Reward Calculation

```

1: Initialization:
2: Initialize satisfaction history queue  $H_{sat}$  (e.g., maxlen=100).
3: Initialize overload history queue  $H_{tr}$  (e.g., maxlen=100).
4: Define base multipliers  $\lambda_{base}^{sat}, \lambda_{base}^{tr}$  and base overload penalty  $P_{base}$ .
5: function CALCULATERWARD(current state  $s_t$ , action  $a_t$ )
6: » 1. Calculate Economic Profit
7:    $\Pi_t \leftarrow \text{CalculateEconomicProfit}(s_t, a_t)$ 
8:    $R_t \leftarrow \Pi_t$ 
9:   » 2. Calculate Adaptive Satisfaction Penalty
10:   $\bar{S}_{hist} \leftarrow \text{Average}(H_{sat})$ 
11:   $\lambda_t^{sat} \leftarrow \lambda_{base}^{sat} \cdot (1 - \bar{S}_{hist})^2$ 
12:  Let  $\mathcal{E}_{\text{depart}}$  be the set of EVs departing at timestep  $t$ .
13:  if  $\mathcal{E}_{\text{depart}}$  is not empty then
14:     $S_{min} \leftarrow \min_{k \in \mathcal{E}_{\text{depart}}} S_k$ 
15:    if  $S_{min} < 0.95$  then
16:       $P_t^{sat} \leftarrow \lambda_t^{sat} \cdot (1 - S_{min})$ 
17:       $R_t \leftarrow R_t - P_t^{sat}$ 
18:    end if
19:  end if
20:  » 3. Calculate Adaptive Transformer Overload Penalty
21:   $F_{hist}^{tr} \leftarrow \text{Frequency of overloads in } H_{tr}$ 
22:   $\lambda_t^{tr} \leftarrow \lambda_{base}^{tr} \cdot F_{hist}^{tr}$ 
23:   $O_t \leftarrow \sum_{j=1}^{N_T} \max(0, P_j^{\text{total}}(t) - P_j^{\text{max}})$ 
24:  if  $O_t > 0$  then
25:     $P_t^{tr} \leftarrow P_{base} + \lambda_t^{tr} \cdot O_t$ 
26:     $R_t \leftarrow R_t - P_t^{tr}$ 
27:  end if
28:  » 4. Update Historical Data
29:   $\bar{S}_{curr} \leftarrow \text{Average satisfaction of currently connected EVs}$ 
30:  Append  $\bar{S}_{curr}$  to  $H_{sat}$ 
31:  Append (1 if  $O_t > 0$  else 0) to  $H_{tr}$ 
32:  return  $R_t$ 
33: end function

```

Economic Profit

The foundation of the reward signal is the direct, instantaneous economic profit, Π_t . This component provides an unambiguous incentive for the agent to exploit market dynamics by encouraging charging during low-price periods and discharging (V2G) during high-price periods.

$$\Pi_t = \sum_{i=1}^{N_{ev}} \left(C_t^{\text{sell}} \cdot P_{i,t}^{\text{dis}} - C_t^{\text{buy}} \cdot P_{i,t}^{\text{ch}} \right) \Delta t \quad (3.11)$$

where N_{ev} is the number of connected EVs, C_t^{sell} and C_t^{buy} are the electricity selling and buying prices, and $P_{i,t}^{\text{dis}}$ and $P_{i,t}^{\text{ch}}$ are the discharging and charging powers for EV i at timestep t .

Adaptive User Satisfaction Penalty

The penalty for failing to meet user charging demands, P_t^{sat} , adapts based on the system's recent performance. The environment maintains a short-term memory of user satisfaction, from which an average historical score, \bar{S}_{hist} , is calculated. A *satisfaction severity multiplier*, λ_t^{sat} , is then computed, which grows quadratically as the historical average satisfaction drops. This ensures that as performance degrades, the consequences of new failures become substantially more severe.

$$\lambda_t^{\text{sat}} = \lambda_{\text{base}}^{\text{sat}} \cdot (1 - \bar{S}_{hist})^2 \quad (3.12)$$

where $\lambda_{\text{base}}^{\text{sat}}$ is a base scaling factor (e.g., 20.0). A penalty is only applied if the satisfaction score of any user, S_k , falls below a critical threshold (e.g., 95%). The magnitude of the penalty is the product of the adaptive multiplier and the current satisfaction deficit.

$$P_t^{\text{sat}} = \begin{cases} \lambda_t^{\text{sat}} \cdot (1 - \min_k S_k) & \text{if } \min_k S_k < 0.95 \\ 0 & \text{otherwise} \end{cases} \quad (3.13)$$

This mechanism establishes a powerful feedback loop: an isolated failure in a well-performing system results in a mild penalty, whereas persistent failures trigger rapidly escalating penalties that compel the agent to correct its policy.

Adaptive Transformer Overload Penalty

The transformer overload penalty, P_t^{tr} , operates on a similar adaptive principle, responding to the recent frequency of overloads, F_{hist}^{tr} . This frequency is tracked over the same historical window and directly drives the computation of a linear *overload severity multiplier*, λ_t^{tr} .

$$\lambda_t^{\text{tr}} = \lambda_{\text{base}}^{\text{tr}} \cdot F_{hist}^{\text{tr}} \quad (3.14)$$

where $\lambda_{\text{base}}^{\text{tr}}$ is a base scaling factor (e.g., 50.0). If the total power drawn from any transformer j , $P_j^{\text{total}}(t)$, exceeds its limit, P_j^{max} , a penalty is applied. This penalty consists of a small, fixed base amount P_{base} plus the adaptive component, which scales with the magnitude of the current overload.

$$P_t^{\text{tr}} = P_{\text{base}} + \lambda_t^{\text{tr}} \cdot \sum_{j=1}^{N_T} \max(0, P_j^{\text{total}}(t) - P_j^{\text{max}}) \quad (3.15)$$

This structure enforces a critical lesson: while an occasional, minor overload might be tolerable in pursuit of high profit, habitual overloading becomes increasingly costly as penalties escalate, forcing the agent to respect physical constraints.

Rationale and Significance

This history-based adaptive reward function represents a significant departure from static or purely state-based approaches. By making penalty weights a function of recent performance, we provide a more sophisticated learning signal. The agent is not excessively punished for isolated, exploratory actions that might lead to minor constraint violations. Instead, it is strongly discouraged from developing policies that produce chronic system failures. This approach mirrors realistic management objectives: maintain high performance on average and react decisively only when performance trends begin to deteriorate. The resulting reward structure guides the agent to discover policies that balance economic objectives with operational reliability, achieving an intelligent equilibrium between profit ambition and system safety.

Implementation Details This reward function, along with a suite of other strategies, is implemented in the `ev2gym/rl_agent/reward.py` module. The main experimentation script, `run_experiments.py`, allows the user to dynamically select the reward function for any given training run. The `FastProfitAdaptiveReward` function uses `collections.deque` objects, attached to the environment instance at runtime, to efficiently maintain a sliding window of recent performance for both satisfaction and overload events. This method is computationally efficient, avoiding complex state-dependent calculations in favor of simple updates to the historical data queues.

3.16 Online MPC Formulation (PuLP Implementation)

The Model Predictive Control (MPC) implemented with PuLP solves a profit maximization problem at each control interval over a finite prediction horizon H . This formulation is designed for online, real-time control, where decisions are made based on the current system state and future predictions. This approach is often termed an "implicit" MPC because the control law is not pre-computed; instead, it is found implicitly by solving a full optimization problem at every control interval. The logic is formally detailed in Algorithm 6.

Implementation Details This online controller is implemented as the `OnlineMPC_Solver` class within the `ev2gym/baselines/pulp_mpc.py` module. At each invocation of its `get_action` method, it dynamically constructs the full Mixed-Integer Linear Program (MILP) described below using the **PuLP** modeling library. PuLP acts as a high-level modeling interface, which then calls an underlying solver. The problem is then solved using the default CBC (COIN-OR Branch and Cut) solver, an open-source solver capable of handling MILPs.

Algorithm 6 Online Model Predictive Control (MILP)

```

1: function GETACTION( $E_{\text{initial}}$ ,  $k_{\text{dep}}$ ,  $c_{\text{buy}}$ ,  $c_{\text{sell}}$ ,  $H$ ,  $N_c$ )
2:   Inputs: Current energy states  $E_{\text{initial}}$ , departure times  $k_{\text{dep}}$ , price vectors
       $c_{\text{buy}}$ ,  $c_{\text{sell}}$ , prediction horizon  $H$ , control horizon  $N_c$ .
3:   Initialize Problem: Create a new MILP problem for profit maximization.
4:   Define Variables for  $i \in \text{CS}$ ,  $k \in [0, H - 1]$ :
5:      $P_{i,k}^{\text{ch}}, P_{i,k}^{\text{dis}} \in \mathbb{R}^+$                                  $\triangleright$  Continuous power variables
6:      $E_{i,k} \in \mathbb{R}^+$                                           $\triangleright$  Continuous energy state variables
7:      $z_{i,k} \in \{0, 1\}$                                       $\triangleright$  Binary charge/discharge mode variables
8:   Define Objective Function:
9:     Profit  $\leftarrow \sum_{k=0}^{H-1} \sum_{i \in \text{CS}} \left[ (c_{\text{user}}^{\text{user}} - c_k^{\text{buy}} - c^{\text{deg}}) P_{i,k}^{\text{ch}} + (c_k^{\text{sell}} - c^{\text{deg}}) P_{i,k}^{\text{dis}} \right] \Delta t$ 
10:    Set objective to max(Profit).
11:    Add Constraints for  $i \in \text{CS}$ ,  $k \in [0, H - 1]$ :
12:      if  $k = 0$  then
13:         $E_{i,k} = E_{\text{initial},i} + (\eta_{\text{ch}} P_{i,k}^{\text{ch}} - \frac{1}{\eta_{\text{dis}}} P_{i,k}^{\text{dis}}) \cdot \Delta t$ 
14:      else
15:         $E_{i,k} = E_{i,k-1} + (\eta_{\text{ch}} P_{i,k}^{\text{ch}} - \frac{1}{\eta_{\text{dis}}} P_{i,k}^{\text{dis}}) \cdot \Delta t$ 
16:      end if
17:       $0 \leq P_{i,k}^{\text{ch}} \leq P_i^{\text{ch,max}} \cdot z_{i,k}$ 
18:       $0 \leq P_{i,k}^{\text{dis}} \leq P_i^{\text{dis,max}} \cdot (1 - z_{i,k})$ 
19:       $E_i^{\text{min}} \leq E_{i,k} \leq E_i^{\text{max}}$ 
20:      if  $k = k_{\text{dep},i}$  then
21:         $E_{i,k} \geq E_i^{\text{des}}$ 
22:      end if
23:       $\sum_{i \in \text{CS}} (P_{i,k}^{\text{ch}} - P_{i,k}^{\text{dis}}) \leq P^{\text{tr,max}}$ 
24:    Solve Problem:
25:    solution  $\leftarrow \text{SOLVEMILP}(\text{Problem})$ 
26:    if solution is Optimal then
27:      Extract action plan  $\{a_k^*\}_{k=0}^{N_c-1}$  from solution.
28:      return action plan
29:    else
30:      return empty plan or default action
31:    end if
32:  end function

```

3.16.1 Mathematical Formulation

The mathematical structure of the optimization problem solved in Algorithm 6 is a classic **Mixed-Integer Linear Program (MILP)**. This classification is justified as follows:

- **Linear Objective Function:** The objective function is a linear combination of the continuous power variables P^{ch} and P^{dis} .
- **Linear Constraints:** All system constraints, including energy dynamics,

power limits, and state of energy bounds, are formulated as linear equations or inequalities.

- **Mixed-Integer Variables:** The formulation employs both continuous variables (e.g., $P_{i,k}^{\text{ch}}$, $E_{i,k}$) and discrete, binary integer variables ($z_{i,k}$). The binary variables are essential for modeling the logical decision to either charge or discharge at any given time step.

3.17 Lyapunov-based Adaptive Horizon MPC

A key enhancement developed in this work is the **Lyapunov-based Adaptive Horizon MPC**, which aims to reduce the computational burden of the online MPC while retaining its optimality and stability guarantees. The controller dynamically adjusts its prediction horizon H_t based on the stability of the system, which is formally assessed using a Lyapunov function. A Lyapunov function $V(x)$ is a scalar function that measures the system's deviation from a desired equilibrium state. For the V2G system, we define it as the sum of squared errors from the desired final energy state:

$$V(E_t) = \sum_{i \in \text{EVs}} (E_{i,t} - E_i^{\text{des}})^2 \quad (3.16)$$

The adaptive control logic, which wraps either the MILP or MIQP solver, is detailed in Algorithm 8.

Algorithm 7 Lyapunov-based Adaptive Horizon MPC

```

1: Initialization:
2: Initialize current horizon  $H_{\text{current}} \leftarrow H_{\max}$ .
3: Define horizon bounds  $H_{\min}, H_{\max}$  and convergence rate  $\alpha$ .
4: Initialize action plan  $\mathcal{A} \leftarrow \emptyset$ .
5: function GETADAPTIVEACTION(current state  $s_t$ )
6:   if action plan  $\mathcal{A}$  is not empty then
7:      $a_t \leftarrow$  Pop first action from  $\mathcal{A}$ .
8:     return  $a_t$ .
9:   end if
10:  ▷ Plan is empty, re-optimization is needed
11:   $E_t \leftarrow$  Get current energy states from  $s_t$ .
12:   $V(E_t) \leftarrow \sum_i (E_{i,t} - E_i^{\text{des}})^2$ .
13:  ▷ Solve MPC with the current horizon
14:  solution  $\leftarrow$  SOLVEMPC( $s_t, H_{\text{current}}$ ) ▷ Using MILP or MIQP solver
15:  if solution is Optimal then
16:    Extract optimal first action  $a_t^* = (P_t^{\text{ch},*}, P_t^{\text{dis},*})$ .
17:    Predict next energy state  $E_{t+1}$  using  $a_t^*$ .
18:     $V(E_{t+1}) \leftarrow \sum_i (E_{i,t+1} - E_i^{\text{des}})^2$ . ▷ Verify Lyapunov stability condition
19:    if  $V(E_{t+1}) \leq V(E_t) - \alpha V(E_t)$  then
20:      ▷ Stable: reduce computational load for next cycle
21:       $H_{\text{next}} \leftarrow \max(H_{\min}, H_{\text{current}} - 1)$ .
22:    else
23:      ▷ Not stable enough: increase planning depth
24:       $H_{\text{next}} \leftarrow \min(H_{\max}, H_{\text{current}} + 1)$ .
25:    end if
26:    Extract new action plan  $\mathcal{A}$  from solution.
27:  else
28:    ▷ Solver failed: increase horizon as a safeguard
29:     $H_{\text{next}} \leftarrow \min(H_{\max}, H_{\text{current}} + 1)$ .
30:     $\mathcal{A} \leftarrow$  default safe action.
31:  end if
32:   $H_{\text{current}} \leftarrow H_{\text{next}}$ .
33:   $a_t \leftarrow$  Pop first action from  $\mathcal{A}$ .
34:  return  $a_t$ .
35: end function

```

This intelligent adjustment makes the online MPC more efficient and practical, reducing computation time during stable periods while retaining the ability to perform deep planning when necessary to guarantee system stability and constraint satisfaction.

Bibliography

- [1] Feyijimi Adegbohun et al. "A Review of Bidirectional Charging Grid Support Applications and Control". In: *Energies* 17.6 (2024), p. 1320. doi: [10.3390/en17061320](https://doi.org/10.3390/en17061320).
- [2] Fayiz Alfaverh, Mouloud Denai, and Yichuang Sun. "Optimal vehicle-to-grid control for supplementary frequency regulation using deep reinforcement learning". In: *Applied Energy* 325 (2022), p. 119881. doi: [10.1016/j.apenergy.2022.119881](https://doi.org/10.1016/j.apenergy.2022.119881).
- [3] Dou An, Feifei Cui, and Xun Kang. "Optimal scheduling for charging and discharging of electric vehicles based on deep reinforcement learning". In: *Frontiers in Energy Research* 11 (2023), p. 1273820. doi: [10.3389/fenrg.2023.1273820](https://doi.org/10.3389/fenrg.2023.1273820).
- [4] Alberto Bemporad. "Explicit Model Predictive Control". In: *Springer Handbook of Automation* (2013), pp. 883–898.
- [5] Alberto Bemporad and Carlo Filippi. "Suboptimal Explicit MPC via Approximate Multiparametric Quadratic Programming". In: *Proceedings of the 40th IEEE Conference on Decision and Control* (Dec. 2001), pp. 4851–4856.
- [6] Christoph R. Birkl et al. "Degradation diagnostics for lithium ion cells". In: *Journal of Power Sources* 341 (2017), pp. 373–386.
- [7] Francesca Bisetto. "La Duck Curve e la scomposizione della stagionalità dei consumi elettrici. Aspetti teorici e modelli statistici". Dipartimento di Scienze Statistiche, Correlatore: Luigi Grossi. Tesi di laurea magistrale. Padova: Università degli Studi di Padova, 2023.
- [8] Francesco Borrelli, Alberto Bemporad, and Manfred Morari. *Predictive Control for Linear and Hybrid Systems*. Cambridge University Press, 2017.
- [9] Greg Brockman et al. "OpenAI Gym". In: *arXiv preprint arXiv:1606.01540* (2016). doi: [10.48550/arXiv.1606.01540](https://doi.org/10.48550/arXiv.1606.01540).
- [10] E.F. Camacho and C. Bordons. *Model Predictive Control*. Springer Science & Business Media, 2013.
- [11] Viorica Rozina Chifu et al. "A Deep Q-Learning based Smart Scheduling of EVs for Demand Response in Smart Grids". In: *arXiv preprint arXiv:2401.02653* (2024). doi: [10.48550/arXiv.2401.02653](https://doi.org/10.48550/arXiv.2401.02653).
- [12] European Commission. *Fit for 55: Delivering the EU's 2030 Climate Target*. 2021. URL: <https://eur-lex.europa.eu/legal-content/EN/TXT/HTML/?uri=CELEX%3A52021DC0550>.

- [13] C. R. Cutler and B. L. Ramaker. "Dynamic Matrix Control – A Computer Control Algorithm". In: *Proceedings of the Joint Automatic Control Conference*. Paper No. WP5-B. American Control Conference. San Francisco, USA, 1980.
- [14] Englberger. "Electric vehicle multi-use: Optimizing multiple value streams using mobile storage systems in a vehicle-to-grid context". In: *Applied Energy* (2021). doi: [10.1016/j.apenergy.2021.117138](https://doi.org/10.1016/j.apenergy.2021.117138).
- [15] Gianluca Faggio. "Design and Testing of Online and Offline Optimization Algorithms for Vehicle-to-Grid (V2G) Industrial Applications". MA thesis. Politecnico di Milano, 2023.
- [16] Kilian Freitag et al. "Curriculum Reinforcement Learning for Complex Reward Functions". In: *arXiv preprint arXiv:2410.16790* (2024).
- [17] Scott Fujimoto, Herke van Hoof, and David Meger. "Addressing Function Approximation Error in Actor-Critic Methods". In: *Proceedings of the 35th International Conference on Machine Learning (ICML)*. 2018. URL: <https://arxiv.org/abs/1802.09477>.
- [18] Shuifu Gu, Kejun Qian, and Yongbiao Yang. "Optimization of Electric Vehicle Charging and Discharging Strategies Considering Battery Health State: A Safe Reinforcement Learning Approach". In: *World Electric Vehicle Journal* 16.5 (2025), p. 286. doi: [10.3390/wevj16050286](https://doi.org/10.3390/wevj16050286).
- [19] Tuomas Haarnoja et al. "Soft Actor-Critic Algorithms and Applications". In: *arXiv preprint arXiv:1812.05905* (2019). URL: <https://arxiv.org/abs/1812.05905>.
- [20] Tuomas Haarnoja et al. "Soft actor-critic: Off-policy maximum entropy deep reinforcement learning with a stochastic actor". In: *International Conference on Machine Learning*. PMLR. 2018, pp. 1861–1870.
- [21] Sinan Ibrahim et al. "Comprehensive Overview of Reward Engineering and Shaping in Advancing Reinforcement Learning Applications". In: *IEEE Access* PP.99 (2024), pp. 1–1. doi: [10.1109/ACCESS.2024.3504735](https://doi.org/10.1109/ACCESS.2024.3504735). URL: <https://arxiv.org/abs/2408.10215>.
- [22] Benjamin Karg and Sergio Lucia. "Efficient representation and approximation of model predictive control laws via deep learning". In: *IEEE Transactions on Cybernetics* 50.9 (2020), pp. 3866–3878. doi: [10.1109/TCYB.2020.2999556](https://doi.org/10.1109/TCYB.2020.2999556).
- [23] Arthur J Krener. "Adaptive Horizon Model Predictive Control". In: *arXiv preprint arXiv:1602.08619* (2016). arXiv: [1602.08619](https://arxiv.org/abs/1602.08619) [math.OC].
- [24] Arsenii Kuznetsov et al. "Controlling Overestimation Bias with Truncated Mixture of Continuous Distributional Quantile Critics". In: *Proceedings of the 37th International Conference on Machine Learning (ICML)*. 2020. URL: <https://proceedings.mlr.press/v119/kuznetsov20a/kuznetsov20a.pdf>.
- [25] Timothy P Lillicrap et al. "Continuous control with deep reinforcement learning". In: *arXiv preprint arXiv:1509.02971* (2015).

- [26] Ding Liu et al. "Deep reinforcement learning for charging scheduling of electric vehicles considering distribution network voltage stability". In: *Sensors* 23.3 (2023), p. 1618. doi: [10.3390/s23031618](https://doi.org/10.3390/s23031618).
- [27] Horia Mania, Aurelia Guy, and Benjamin Recht. "Simple Random Search Provides a Competitive Approach to Reinforcement Learning". In: *arXiv preprint arXiv:1803.07055* (2018). URL: <https://arxiv.org/abs/1803.07055>.
- [28] D. Q. Mayne et al. "Constrained model predictive control: Stability and optimality". In: *Automatica* 36.6 (2000), pp. 789–814. doi: [10.1016/S0005-1098\(99\)00214-9](https://doi.org/10.1016/S0005-1098(99)00214-9).
- [29] Carlos A Minchala-Ávila, Paúl Arévalo, and Diego Ochoa-Correa. "A Systematic Review of Model Predictive Control for Robust and Efficient Energy Management in Electric Vehicle Integration and V2G Applications". In: *Modelling* 6.1 (2025), p. 20. doi: [10.3390/modelling6010020](https://doi.org/10.3390/modelling6010020).
- [30] Volodymyr Mnih et al. "Asynchronous Methods for Deep Reinforcement Learning". In: *Proceedings of the 33rd International Conference on Machine Learning (ICML)*. 2016, pp. 1928–1937. URL: <https://arxiv.org/abs/1602.01783>.
- [31] Andrew Y Ng, Daishi Harada, and Stuart Russell. "Policy invariance under reward transformations: Theory and application to reward shaping". In: *University of California, Berkeley* (1999).
- [32] Stylianos Orfanoudakis et al. "EV2Gym: A Flexible V2G Simulator for EV Smart Charging Research and Benchmarking". In: *arXiv preprint arXiv:2404.01849* (2024). doi: [10.48550/arXiv.2404.01849](https://doi.org/10.48550/arXiv.2404.01849).
- [33] Rey Pocius et al. "Comparing Reward Shaping, Visual Hints, and Curriculum Learning". In: *Proceedings of the AAAI Conference on Artificial Intelligence* (2019).
- [34] Dajun Qiu et al. "Reinforcement learning for vehicle-to-grid: A review". In: *Renewable and Sustainable Energy Reviews* 167 (2022), p. 112702.
- [35] Dawei Qiu et al. "Reinforcement learning for electric vehicle applications in energy management: A review". In: *Renewable and Sustainable Energy Reviews* 163 (2023), p. 112443. doi: [10.1016/j.rser.2022.112443](https://doi.org/10.1016/j.rser.2022.112443).
- [36] Jacques Richalet et al. "Model predictive heuristic control: Applications to industrial processes". In: *Automatica* 14.5 (1978), pp. 413–428. doi: [10.1016/0005-1098\(78\)90001-8](https://doi.org/10.1016/0005-1098(78)90001-8).
- [37] Mohammad Sadeghi. "Cost and power loss aware coalitions under uncertainty in transactive energy systems". In: *Université d'Ottawa / University of Ottawa* (2022). PhD Thesis.
- [38] Gabriel Antonio Salvatti et al. "Electric Vehicles Energy Management with V2G/G2V Multifactor Optimization of Smart Grids". In: *Energies* 13.5 (2020), p. 1191. doi: [10.3390/en13051191](https://doi.org/10.3390/en13051191).

- [39] Tom Schaul et al. "Prioritized experience replay". In: *arXiv preprint arXiv:1511.05952* (2015). doi: [10.48550/arXiv.1511.05952](https://doi.org/10.48550/arXiv.1511.05952).
- [40] John Schulman et al. "Proximal Policy Optimization Algorithms". In: *Proceedings of the 34th International Conference on Machine Learning (ICML)*. 2017, pp. 3371–3380. URL: <https://arxiv.org/abs/1707.06347>.
- [41] John Schulman et al. "Trust Region Policy Optimization". In: *Proceedings of the 32nd International Conference on Machine Learning (ICML 37)* (2015), pp. 1889–1897. URL: <https://proceedings.mlr.press/v37/schulman15.html>.
- [42] G. Srihari et al. "Integration of electric vehicle into smart grid: a meta heuristic algorithm for energy management between V2G and G2V". In: *Frontiers in Energy Research* 12 (2024), p. 1357863. doi: [10.3389/fenrg.2024.1357863](https://doi.org/10.3389/fenrg.2024.1357863).
- [43] Richard S. Sutton and Andrew G. Barto. *Reinforcement Learning: An Introduction*. Second edition, in progress. A Bradford Book, c. 2014, 2015. Cambridge, Massachusetts; London, England: The MIT Press, 2015.
- [44] Ahmad Tavakoli et al. "Impacts of grid integration of solar PV and electric vehicle on grid stability, power quality and energy economics: a review". In: *IET Energy Systems Integration* 2.3 (2020), pp. 233–245. doi: [10.1049/ietesi.2019.0047](https://doi.org/10.1049/ietesi.2019.0047).
- [45] Jürgen Vetter et al. "Ageing mechanisms in lithium-ion batteries". In: *Journal of Power Sources* 147.1-2 (2005), pp. 269–281.
- [46] David Silver et. al Volodymyr Mnih Koray Kavukcuoglu. "Human-level control through deep reinforcement learning". In: *Nature* 518.7540 (2015), pp. 529–533.
- [47] Mingyu Wang et al. "Multi-Agent Reinforcement Learning is a Sequence Modeling Problem". In: *arXiv preprint arXiv:2205.14953* (2022). URL: <https://arxiv.org/abs/2205.14953>.
- [48] Zhaoyu Wang et al. "An electrical vehicle-assisted demand response management system: A reinforcement learning method". In: *Frontiers in Energy Research* 10 (2022), p. 1071948. doi: [10.3389/fenrg.2022.1071948](https://doi.org/10.3389/fenrg.2022.1071948).
- [49] Corey D. White and K. Max Zhang. "Using vehicle-to-grid technology for frequency regulation and peak-load reduction". In: *Journal of Power Sources* 196.3 (2011), pp. 3972–3980. doi: [10.1016/j.jpowsour.2010.11.010](https://doi.org/10.1016/j.jpowsour.2010.11.010).
- [50] H. Xie. "Reinforcement learning for vehicle-to-grid: A review". In: *ScienceDirect* (2025). doi: [10.1016/j.sciad.2025.100008](https://doi.org/10.1016/j.sciad.2025.100008).
- [51] Na Xu et al. "A Review of Smart Grid Evolution and Reinforcement Learning: Applications, Challenges and Future Directions". In: *Energies* 18.7 (2024), p. 1837. doi: [10.3390/en18071837](https://doi.org/10.3390/en18071837).
- [52] Yubao Zhang, Xin Chen, and Yuchen Zhang. "Transfer deep reinforcement learning-based large-scale V2G continuous charging coordination with renewable energy sources". In: *arXiv preprint arXiv:2210.07013* (2023).